PARTIAL RESPONSE SIGNALING WITH A MAXIMUM LIKELIHOOD SEQUENCE ESTIMATION RECEIVER

by

© N. Chan, B.Eng.

A Thesis
Submitted to the Faculty of Graduate Studies
in Partial Fulfilment of the Requirements
for the Degree
Master of Engineering

McMaster University

December 1980

MASTER OF ENGINEERING (1980)
Electrical and Computer Engineering

McMASTER UNIVERSITY
Hamilton, Ontario

TITLE: Partial Response Signaling with a Maximum Likelihood Sequence Estimation Receiver

AUTHOR: N. Chan, B.Eng. (Concordia University)

SUPERVISOR: Dr. J. B. Anderson

NUMBER OF PAGES: vii, 115

ABSTRACT

This thesis evaluates a bandwidth efficient data transmitting system which is modelled as a PRS system. A maximum likelihood receiver implementing VA is assumed at the receiving end. An algorithm is developed to compute a fundamental performance parameter of the system, called the free distance. 99% energy bandwidth and intersymbol interference (ISI) degradation are used to measure the performance of the system. Nonlinear programming and minimax methods are applied to find the optimal channel codes under different criteria. Three different sets of optimal channel codes have been found; first, the worst-case channel codes in terms of ISI degradation, secondly, the minimum 99% energy bandwidth channel codes and finally the minimum 99% energy bandwidth channel with fixed ISI degradation constraint. Two PRS systems with different pulse shaping filter are considered. First, an ideal low pass filter with minimum Nyquist bandwidth is evaluated for channel lengths up to twelve. Then a spectral raised-cosine filter with roll-off factor equal to one is evaluated for channel lengths up to four. The two PRS systems show that a longer channel can have better performance in consideration of both bandwidth and ISI degradation. The raised cosine filter causes no performance penalty in narrow band channels.

ACKNOWLEDGEMENTS

The author wishes to thank Dr. J. B. Anderson for his guidance and inspiration throughout the course of this program.

The author would also like to express his appreciation from a number of useful discussions with Dr. M. R. M. Rizk.

The financial assistance provided by the Department of Electrical and Computer Engineering is gratefully acknowledged.

Finally, the author also wishes to thank Ms. Linda Hunter for typing this thesis.

TABLE OF CONTENTS

CHAPTER 1

INTRODUCTION

1.1 A. Digital Communication System

Increasing demand for faster, bandwidth efficient and reliable data transmission has caused interest in various signaling schemes and receivers to fulfil these objectives. For instance, on a satellite communication system and a mobile radio system, both the transmission bandwidth and signal to noise ratio (SNR) are of concern. Since the demand for communication is increasing rapidly, the efficient use of channel bandwidth is important to reduce the channel cost directly and conserve the radio spectrum. The immense transmission distance, limited power supply and/or unfavourable channels of these communication systems increase the importance of reliable data transmission with manageable transmission power.

The primary sources of distortion in a high data rate transmission system are intersymbol interference (ISI) and noise. ISI is produced by the tail of a baseband pulse at each symbol period which interferes with the neighbour pulses. Multipath interference has a similar effect.

The purpose of this thesis is to design a bandwidth efficient transmitting system, a so called partial response signaling (PRS) system or correlative encoder. A maximum likelihood (ML) receiver employs the Viterbi Algorithm (VA) to decode the received sequence.

Fig. 1.1 shows the digital communication system model that is used in our work. The input data is assumed to be a sequence of impulse {0,1}, and the transmitting filter correlates the input sequence for spectral shaping to achieve better bandwidth performance. A bandlimited channel corrupted by white Gaussian noise is assumed. On the receiver's side, a matched filter and a maximum likelihood sequence estimator implementing the VA are used as an optimum receiver.

Kabal and Pasupathy [1] presented a detailed study of different PRS schemes from the viewpoint of spectral properties. PRS schemes are based on the idea of introducing some correlation (or ISI) among the data for spectral shaping so as to increase bandwidth efficiency. Since the controlled amount of ISI is introduced to the adjacent symbols in a finite discrete way, the ISI can be eliminated at the receiver by subtracting the previous weighted symbols from present symbol.

Various receiver structures have been proposed to combat the effect of ISI [2]-[5]. One simple structure used in practice is called the linear equalizer. Its performance has been analysed by Lucky [2]. Another kind of receiver that implements a non-linear technique, called the decision feedback equalizer, was analysed by Price [3]. A more recent nonlinear receiver was proposed by Forney [5] which consists of a whitened matched filter, a sampler with symbol rate and a recursive nonlinear processor, called the Viterbi Algorithm (VA). The VA was devised by Viterbi [6] as a decoding algorithm for convolutional codes. Omura [7] pointed out that the VA can be considered as a dynamic programming solution to the decoding problem. Forney [3] and Kobayashi [8] showed that the VA is indeed a maximum likelihood decoder performing maximum likelihood estimation (MLSE) in pulse amplitude modulation (PAM) system with ISI. The performance analysis of a MLSE implementing the VA was reported by Forney [3], [9]. A similar receiver was proposed by Ungerboeck [4], in which the VA was modified to deal with correlative noise directly without a pre-whitening filter. An adaptive scheme for the receiving filter is also proposed in the same paper. Magee [10] proposed another adaptive ML receiver which combines Forney's receiver with a channel estimator so that it can be applied to an unknown slowly time-varying dispersive channel.

Forney showed that the probability of error of MLSE is dominated by the minimum distance at moderate SNR [5]. Magee and Proakis [11] suggested a method to estimate the worst possible performance over a chennel with a fixed energy finite duration pulse response. The results for estimated worst performance were shown for channel lengths up to ten. Anderson and Foschini [12] later provided a procedure for computing the minimum distance for classes of a few hundred states. A combined functional analysis and computer search approach was used to find the minimum distance. Their results indicated that Magee's results [11] were only true for the channel lengths less than seven.

An evaluation on power, bandwidth and complexity in MLSE was done by Wong [13]. The transmitter was modelled as a partial response signaling system, while Forney's receiver was applied at the receiving end. A double dynamic programming technique was developed and used for computation of the minimum distance. Power, bandwidth and complexity were evaluated for channel lengths up to four by plotting the corresponding contour maps.

1.2 Organization of the Thesis

In Chapter 2 of this thesis, the PRS system and its equivalent finite state machine model is discussed. In Chapter 3, a ML receiver proposed by Ungerboeck [4] is presented and compared with Forney's receiver [5].

A modified stack algorithm is derived in Chapter 4 for computation of the minimum distance. Efficiency of the algorithm is discussed and compared with the double dynamic programming method. An optimization technique and the corresponding computer package are introduced in Chapter 5. The computer package is used to solve the problem of optimizing d^2_{free} in Chapter 6 and optimizing bandwidth in Chapter 7 and 8.

Combining the algorithm and technique proposed in Chapter 4 and 5, we have found the worst degradation of the MLSE for channel lengths up to 12 in Chapter 6, while in Chapter 7, we optimize the bandwidth with and without the power constraint for channel lengths up to 10. Finally, a spectral raised cosine function is introduced for pulse shaping rather than the rectangular spectral function used in previous chapters. The same optimization problems in Chapter

6 and 7 are done for the modified system in Chapter 8.

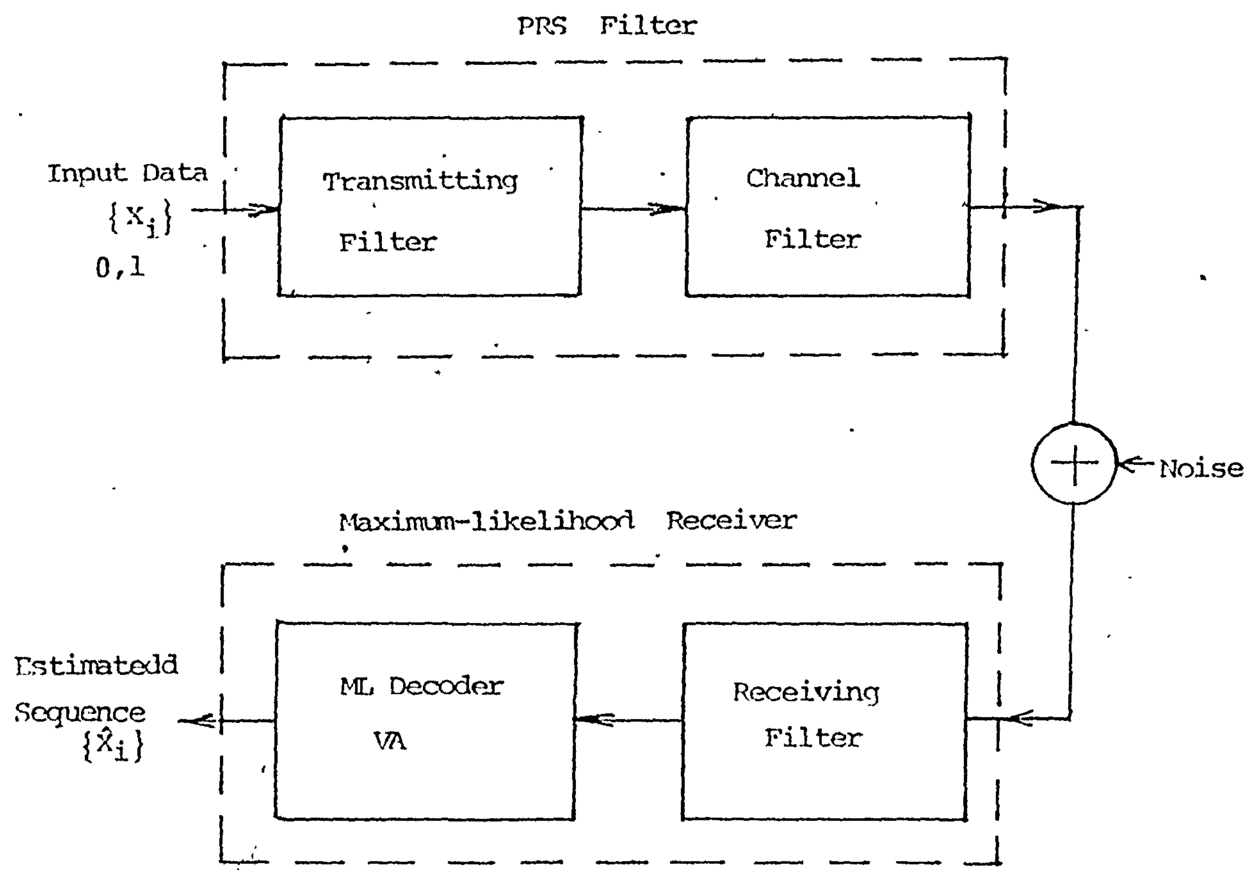

Fig.1.1 A digital communication system.

CHAPTER 2

A BANDWIDTH EFFICIENT SIGNALING SCHEME: PARTIAL RESPONSE SIGNALING

In communication systems, most channels are bandlimited in some sense, so that efficient use of bandwidth is one of the objects of a transmission system. In this chapter, partial response signaling is introduced as a bandwidth efficient signaling scheme.

2.1 Partial Response Signaling System (PRS)

Lender [14] first introduced PRS for data transmission. A PRS system is based on the allowance of a controlled amount of inter-symbol interference (ISI) which is used for spectral shaping so as to redistribute the spectral energy of the signal. Most of the energy concentrates in low frequency region or some other frequency region depending on the correlation introduced among the signals. Since the ISI is known, its effect can be removed or diminished at the receiver. In comparison, a conventional pulse amplitude modulation (PAM) system eliminates ISI by creating a large number of signal levels. A PRS system can achieve high data rate by signaling at a higher rate with fewer levels. Therefore, PRS system will have better error rate performance than the conventional PAM system [2].

A PRS system can be considered as a cascade of a digital transversal filter $F(\omega)$ and a pulse shaping filter $G(\omega)$, as shown in Fig. 2.1 [1].

The digital transversal filter $F(\omega)$ is equivalent to a shift register with K taps. It correlates each input datum with $L = K - 1$ succeeding input data. By controlling the tap coefficients, we can achieve the desired spectrum at the output of $F(\omega)$. In our study, the tap coefficients can be any real numbers.

The transfer function of $F(\omega)$ is

$$F(\omega) \overset{\Delta}{=} \sum_{i=0}^{L} f_i \, e^{-j\omega T} \tag{2.1}$$

where L is number of delay units.

f_i is a tap coefficient

T is one tap delay time which is equal to one symbol period.

Its impulse response is

$$F(D) = \sum_{i=0}^{L} f_i \, D^i \tag{2.2}$$

where D is the Huffman's delay operator [5].

$F(\omega)$ is a periodic function with period 1/T. The analog filter $G(\omega)$ converts the samples Y_K to an analog waveform and in so doing bandlimits the resulting system function, hopefully without too much change to the sample values introduced by $F(D)$. The choice of $G(\omega)$ will be discussed in more detail in next section.

The analogy between PRS and convolutional coding was pointed

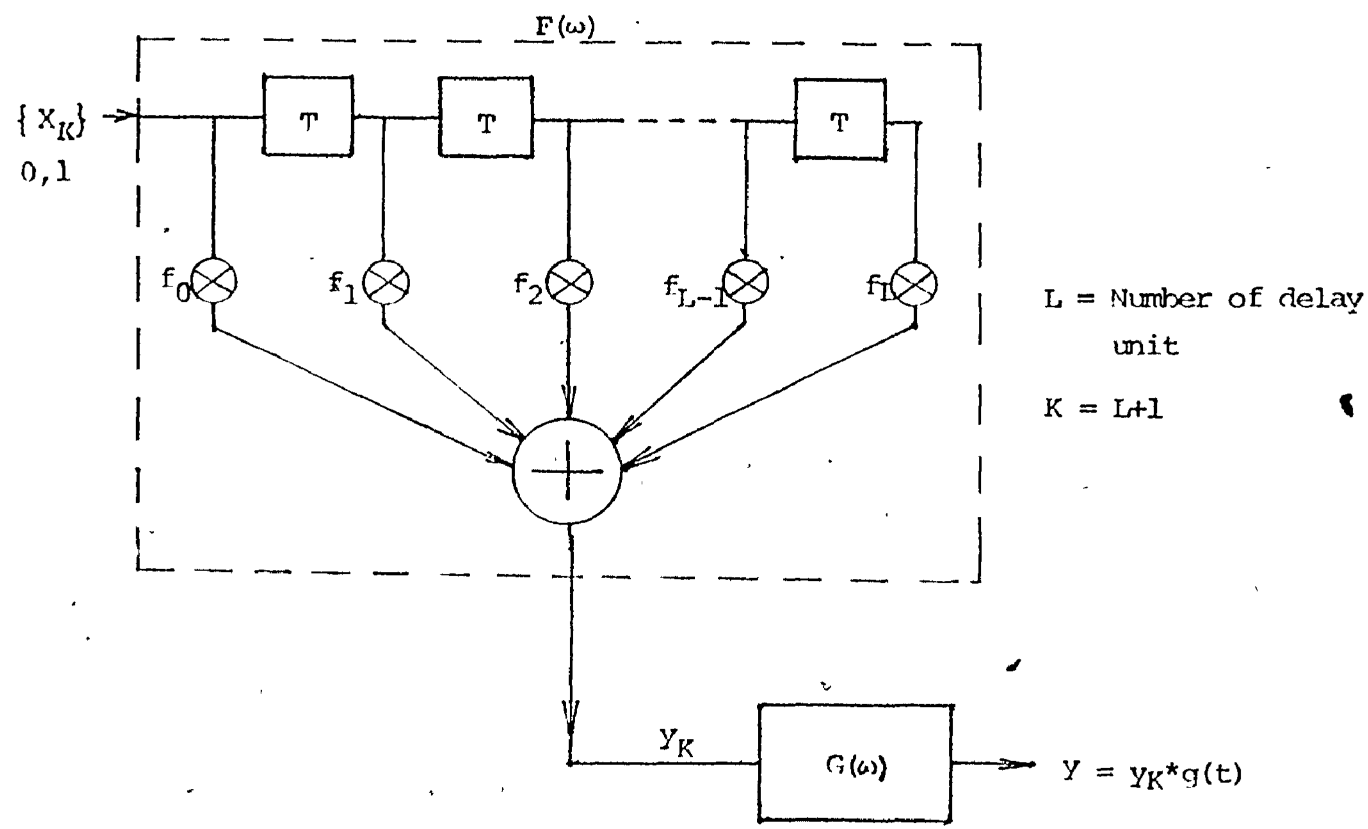

Fig.2.1 A partial response signalling system

out by Kobayashi [14] and Forney [5]. A PRS system can be considered as a simple type of linear finite-state machine defined over the real-number field as opposed to a Galois field over which a binary convolution encoder is defined. Therefore, a PRS system is actually equivalent to a real number convolutional encoder.

2.2 Choice of Pulse Shaping Filter $G(\omega)$

For our work, the requirements of the pulse shaping filter $G(\omega)$ are that $G(\omega)$ must be bandlimited and satisfies Nyquist's first criterion [2].

Nyquist's first criterion states that the impulse response of a function $G(\omega)$ has zeroes at uniformly spaced intervals except for a central peak, i.e.,

$$\begin{aligned} g(KT) &= 0 \quad \text{for} \quad K \neq 0 \\ g(0) &\neq 0 \end{aligned} \tag{2.3}$$

This zero crossing property ensures the sample values introduced by $F(D)$ without change after passing through $G(\omega)$. There exists many different filters that satisfy Nyquist's first criterion. These have different bandwidths, but are all called Nyquist filters. Two different Nyquist filters $G(\omega)$ are considered here.

First, a rectangular spectral function that occupies the minimum Nyquist bandwidth π/T radians with transfer function

$$G(\omega) = \begin{cases} T & |\omega| \leq \pi/T \\ 0 & |\omega| > \pi/T \end{cases} \tag{2.4}$$

Its impulse response is a sinc pulse

$$g(t) = \frac{\sin \pi t/T}{\pi t/T} \tag{2.5}$$

shown in Fig. 2.2.

This filter is equivalent to an ideal low pass filter with cut-off frequency at $\omega = \pi/T$. The discontinuity at $\omega = \pi/T$ causes two disadvantages.

(1) It is physically unrealizable and difficult to approximate.

(2) It results in slow decay of the pulse tail. The pulse response decreases at $1/t$ for large t and a small timing error may introduce large ISI [15].

Another class of Nyquist filter called the spectral raised-cosine function [2] is commonly used in practice. A raised-cosine character consists of a flat amplitude portion and a roll-off portion which has a sinusoidal form.

The transfer function and its impulse response are

$$G(\omega) \begin{cases} T & 0 \leq |\omega| \leq \frac{\pi}{T}(1 - \beta) \\ \frac{T}{2}\{1 - \sin [\frac{T}{2\beta}(\omega - \pi/T)]\} & \frac{\pi}{T}(1 - \beta) \leq |\omega| \leq \frac{\pi}{T}(1 + \beta) \\ 0 & \text{Otherwise} \end{cases} \tag{2.6}$$

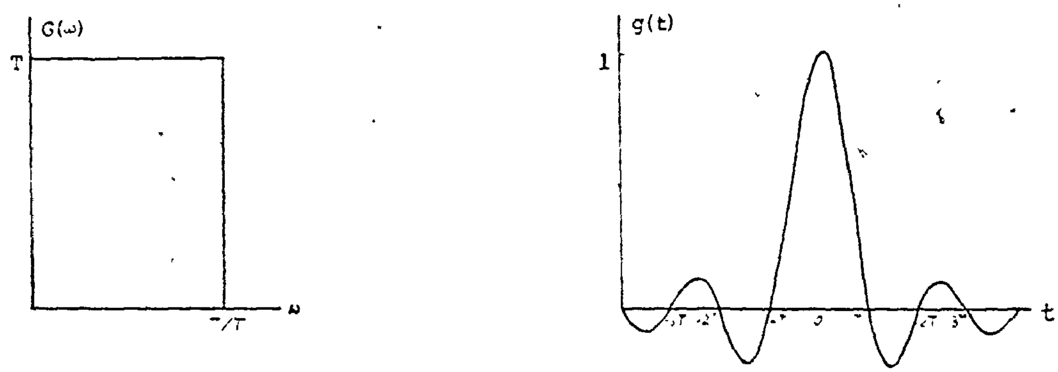

Fig. 2.2 A rectangular function and its impulse response.

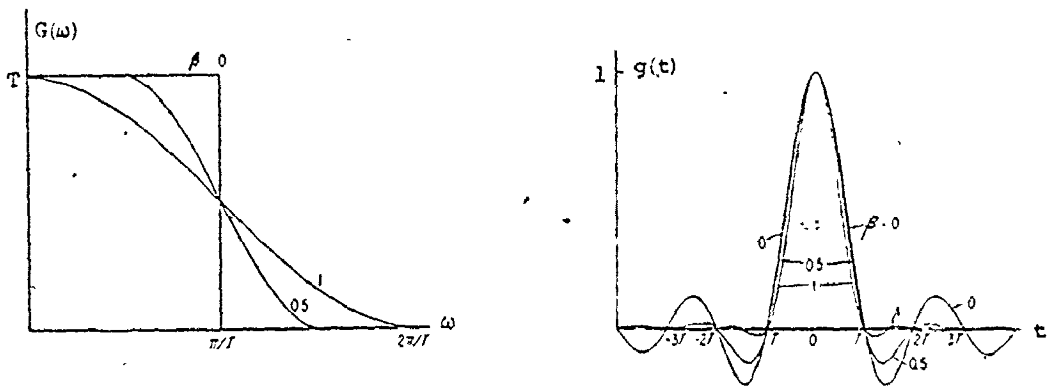

Fig. 2.3 A raised-cosine function and its impulse response.

$$g(t) = \frac{\sin \pi t/T}{\pi t/T} \cdot \frac{\cos\beta\pi t/T}{1-4\beta^2 t^2/T^2} \qquad 0 \le \beta \le 1, \qquad (2.7)$$

where β is called roll-off factor. Plots of $G(\omega)$ and $g(t)$ with three different values of β are shown in Fig. 2.3. For $\beta = 0$, it becomes a rectangular function with minimum bandwidth π/T. As $\beta > 0$, the excess bandwidth is measured by β. When $\beta = 1$, a maximum bandwidth $2\pi/T$ is required. The advantage of the raised-cosine function is that it can allow a moderate timing error without causing serious ISI. This is due to the gradual roll-off of the cut-off frequency, which causes the pulse response to decrease asymptotically as $1/t^3$ [2]. However, since the bandwidth of the raised cosine function is larger than π/T, it will cause aliasing when the output of such system is sampled at the symbol rate T. This degrades performance.

Both Nyquist filters are considered in this work. The rectangular function is first implemented and evaluated in Chapter 6 and 7, whereas the raised-cosine function is treated in Chapter 8.

2.3 Energy and Bandwidth of PRS System

We have mentioned that the bandwidth of a PRS system depends on the choice of $G(\omega)$ function. However, one should notice that energy of the system does not uniformly distribute over the system bandwidth. Adjusting tap coefficients f_i of $F(\omega)$, we can confine most of the energy within the frequency band α. Therefore, the energy carries very little information outside frequency α and can be discarded. 99% energy bandwidth was used by Wong [13], meaning the bandwidth containing 99% of the total energy of the system. Using this definition, we can compute the effective bandwidth required by a PRS system for data transmission.

The energy density of a PRS system is defined as

$$\text{Energy density} \triangleq |F(\omega)\ G(\omega)|^2 \tag{2.8}$$

Then the energy contained within bandwidth α is

$$E(\alpha) \triangleq \frac{1}{2\pi} \int_{-2\pi\alpha}^{2\pi\alpha} |F(\omega)\ G(\omega)|^2 \ d\omega \tag{2.9}$$

where $0 \leq \alpha \leq 1/2T$ Hz for a rectangular function of $G(\omega)$

$0 \leq \alpha \leq 1/T$ Hz for a raised-cosine function of $G(\omega)$.

With (2.9) we can compute the 99% energy bandwidth. That will be done in more detail in Chapter 7.

2.4 Finite State Machine

The PRS digital filter $F(\omega)$ in Fig. 2.1 is a discrete-time shift register. The process is a finite-state discrete-time Markov process [16].

A finite-state discrete-time Markov process is characterized by the states, with the state at any time being given by the L most recent inputs. Define state

$$S_k \triangleq (x_{k-1}, x_{k-2}, \ldots x_{k-L}) \tag{2.10}$$

The number of possible states is m^L for an m-ary input to a shift register with L delay taps.

2.5 Tree and Trellis

A tree is used to represent exhaustively all states and stages of a discrete deterministic process, as shown in Fig. 2.4(a). The nodes of a tree represent the states. Input sequences are indicated by the paths followed in the tree diagram, while outputs are indicated by symbol along the paths.

The trellis diagram is another representation of a finite state machine introduced by Forney [16], as shown in Fig. 2.4(b). It is a tree-like structure with rejoining branches, in which two nodes at the same level in the tree are coalesced if they represent the same output sequence for the same input sequence. It shows the time evolution of the state transitions. The most important property of a trellis diagram is that to every possible state sequence $\{S_k\}$, there corresponds a unique path through the trellis and vice-versa. Therefore an estimation of state sequences is equivalent to a searching of trellis paths.

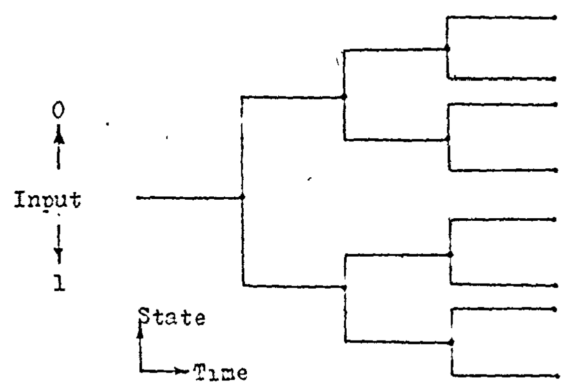

(a) Tree diagram

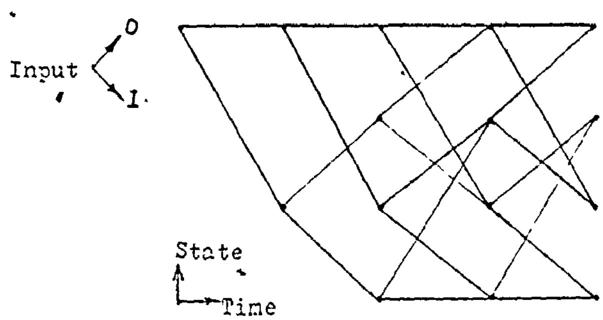

(b) Trellis diagram

Fig. 2.4 Tree and trellis

CHAPTER 3

MAXIMUM LIKELIHOOD RECEIVER

Many different kinds of receivers have been proposed [2]-[5] to combat the effect of ISI, with varying success. The first non-linear receiver structure implementing MLSE to remove ISI was proposed by Forney [5]. The performance analysis of this structure indicated its superiority over the conventional equalization receivers. Ungerboeck [4] later proposed a similar non-linear receiver structure that is considered more general and practical; its performance is the same as Forney's structure [4]. In our work, Ungerboeck's receiver structure is assumed at the receiver end of our digital communication system.

3.1 A Nonlinear Receiver Structure

With a linear carrier-modulated data transmission system, a nonlinear receiver structure implementing MLSE in the presence of ISI was proposed by Ungerboeck [4]. The same receiver structure is applied to our baseband PAM transmission system, as shown in Fig. 3.1. The receiver contains a matched filter followed by a sampler sampling at each symbol period T, which provides a set of sufficient statistics for estimation of the input sequence. Finally, the sampled value of the matched filter output is fed into a nonlinear

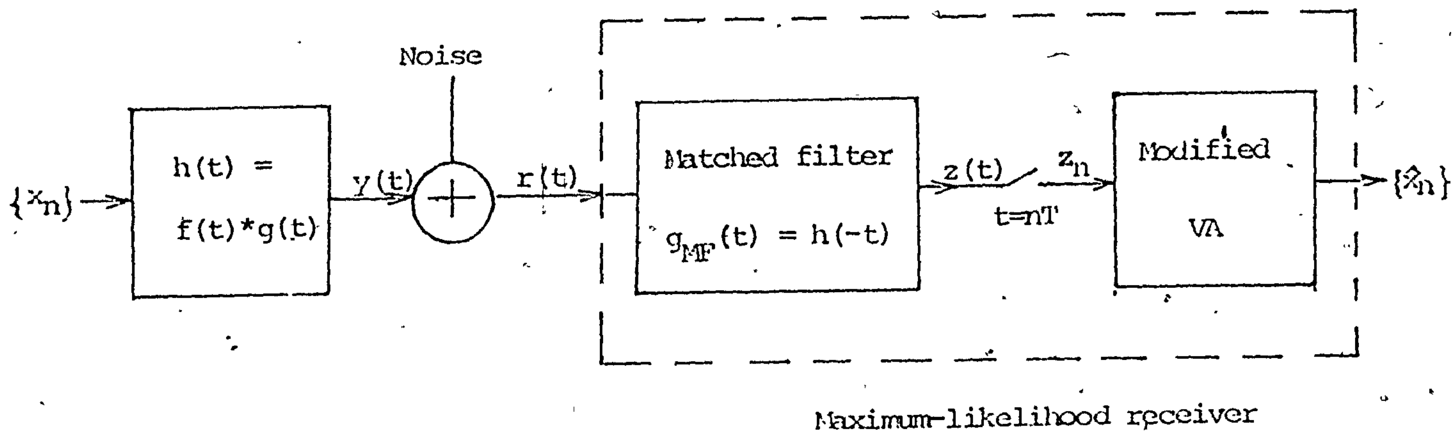

Fig. 3.1 A channel including a nonlinear receiver structure.

recursive processor that performs a modified VA to decode the sequence in an optimum way. The modified VA has the capability to deal with correlated noise as opposed to the original VA used in Forney's structure which can only be applied to statistically independent noise samples. Therefore, a whitening filter is no longer required in Ungerboeck's receiver.

In our work, we assume that the channel is corrupted by white Gaussian noise n(t). Therefore, the observed signal r(t) is

$$r(t) = y(t) + n(t) \tag{3.1}$$

where y(t) is the output of the PRS filter

$$y(t) = \sum_k x_k \, h(t-k) \tag{3.2}$$

where h(t) is the impulse response of the PRS filter.

The observed sequence r(t) is the input of the matched filter which is designed to maximize the SNR. The transfer function of the matched filter is

$$\begin{aligned} G_{MF}(\omega) &= \overline{H}(\omega) \qquad (3.3) \\ &= \overline{F}(\omega)\,\overline{G}(\omega) \end{aligned}$$

where $^{-}$ represents complex conjucate.

The impulse response of matched filter is

$$\begin{aligned} g_{MF}(t) &= h(-t) \\ &= f(-t) * g(-t) \qquad (3.4) \end{aligned}$$

where $*$ represents convolution.

The output of the matched filter is sampled and has sample value Zn.

$$\begin{aligned} Zn &= g_{MF}(t) * r(t) \mid t = nT \\ &= g_{MF}(t) * (y(t) + n(t)) \mid t = nT \\ &= (g_{MF}(t) * y(t) + g_{MF}(t) * n(t)) \mid t = nT \\ &= (g_{MF}(t) * \sum_{1} x_{n-1}\, h(t)) \mid t = nT + n_n \\ &= \sum_{\ell} x_{n-1}\, s_{\ell} + n_n \end{aligned} \tag{3.4}$$

where $s_{\ell} = g_{MF}(t) * h(t) \mid t = \ell T$. (3.5)

s_{ℓ} is called the sampled value of the overall PRS and receiving matched filter, or it can be considered as the autocorrelation function of the overall channel. Here n_n is the noise sample that is correlated after passing through the matched filter.

3.2 Maximum Likelihood Sequence Estimation for PRS Systems

Maximum likelihood sequence estimation (MLSE) is defined as the choice of a transmitted input sequence $\hat{x}_n$ that maximizes the probability density function $P[r(t)/\{x_n\}]$. We express the probability density function as the likelihood function L.

$$L \triangleq P[r(t)/\{x_n\}] \tag{3.6}$$

From (3.1), we have the noise term

$$n(t) = r(t) - y(t)$$

$$= r(t) - \sum_{nT\varepsilon I} x_n h(t-nT) \qquad (3.7)$$

where I is time interval that the receiver observes r(t).

Since we have assumed the noise added in the channel is White Gaussian noise, the likelihood function becomes [4].

$$L = P[r(t),\ t\varepsilon I/\{x_n\}]$$

$$= p_n[n(t)]$$

$$\doteq c\cdot \exp\{-\frac{1}{2N_0} \int_I [n(t)]^2\, dt\} \qquad (3.8)$$

where c is independent of x_n.

Substituting (3.7) into (3.8) we have

$$L = c\cdot\exp\{-\frac{1}{2No} \int_I [r(t) - \sum_{nT\varepsilon I} x_i h(t-iT)]^2\, dt \qquad (3.9)$$

Multiple out the terms and discard those terms that are independent of $\{x_n\}$, (3.9) becomes

$$L = \exp\{\frac{1}{2No} \sum_{nT\varepsilon I} (2x_n Z_n) - \sum_{iT\varepsilon I} \sum_{kT\varepsilon I} x_i s_{i-k} x_k\} \qquad (3.10)$$

where Zn and s_ℓ is defined by (3.4) and (3.5).

Because the natural log function is a monotone function, the maximization of L is equivalent to maximizing ln(L). Therefore, a MLSE is to find the maximum of

$$\Gamma_n(\{x_n\}) \triangleq \sum_{nT\varepsilon I} 2x_n Z_n - \sum_{iT\varepsilon I} \sum_{kT\varepsilon I} x_i s_{i-k} s_k \tag{3.11}$$

Γ_n is also called a "metric value" of $\{x_n\}$.

3.3 Modified Viterbi Algorithm

One way to solve (3.11) is to search among all possible input sequences $\{x_n\}$ and select the one that maximizes Γ_n. This brute force method can never be applied in practice because of the extremely large number of possible input sequences $\{x_n\}$. Formulating (3.11) into recursive form, we can apply dynamic programming techniques [13] to select the optimum sequence in a much more efficient way.

The autocorrelation function is symmetric i.e. $s_\ell = s_{-\ell}$ and rewrite (3.11) into recursive form, we have

$$\Gamma_n(\{x_n\}) = \Gamma_{n-1}(\{x_{n-1}\}) + x_n \{2Z_n - s_o x_n - 2 \sum_{k\leq n-1} s_{n-k} x_k\} \tag{3.12}$$

$$= \Gamma_{n-1}(\{x_{n-1}\}) + x_n \{2Z_n - s_o x_n - 2 \sum_{\ell=1}^{L} s_\ell x_{n-\ell}\} \tag{3.13}$$

where L is the constraint length of the ISI or equivalently the channel memory length.

In a PRS system, the input sequence $\{x_n\}$ and the state sequence $\{S_n\}$ corresponds one to one. The estimation of an input sequence is then equivalent to the estimation of a state sequence and it is usually more convenient to search a state sequence because these sequences have a trellis structure. Therefore, we rewrite (3.13) as a function of state,

$$\Gamma_n (S_n) = \Gamma_{n-1} (S_{n-1}) + x_n (2Z_n) - F(S_{n-1}, S_n) \tag{3.14}$$

where
$$F(S_{n-1}, S_n) = x_n s_o x_n + 2 \sum_{l=1}^{L} s_l \, x_{n-l} \,. \tag{3.15}$$

We can apply (3.14) and the dynamic programming concept to derive the modified VA for optimum decoding. A dynamic programming approach is actually an efficient search along a trellis. For instance, in a trellis of depth N, instead of choosing one path through the trellis that gives a maximum metric, the selection is decomposed into N incremental choices. For every depth $n \geq K$, we select a path among the m paths terminating at the same state U, that gives the maximum metric. State U is called the survivor state and the corresponding metric is called the survivor metric. There are m^L survivors at each stage. Mathematically, the survivor can be represented as

$$\hat{\Gamma}_n (U) = \max \{2x_n Z_n - F(V_i, U), \text{ for each } 1 \leq i \leq m,$$

$$\text{such that } \delta(V_i, x_n) = U\} \tag{3.16}$$

where $\delta(V, x_n)$ means the state transition of V with input data x_n.

Therefore, we select one survivor from m different paths that merge at the same state and each state will have one survivor. We can represent the recursive equation (3.14) in terms of survivor sequence.

$$\hat{\Gamma}_n(\hat{S}_n) = \hat{\Gamma}_{n-1}(\hat{S}_{n-1}) + \max_{\hat{S}_{n-1} \to S_n} \{2x_n Z_n - F(\hat{S}_{n-1}, S_n)\} \tag{3.17}$$

where $\hat{S}_{n-1}$ is the survivor state sequence from time zero to time n-1.

The modified VA is just the implementation of the nonlinear recursive equation (3.17).

Considering of complexity of this modified VA, we estimate the memory and computation requirements to implement the algorithm.

In terms of memory, $2m^L$ memory locations are required to store previous and present optimal value metrics $\hat{\Gamma}_n(\hat{S}_n)$ and $\hat{\Gamma}_{n-1}(\hat{S}_{n-1})$. $F(\hat{S}_{n-1}, S_n)$ may be computed in advance and stored for table look-up; then it requires m^{L+1} memory to store the table. In terms of computation, in each symbol period there are m^{L+1} operations, each involving a multiplication $2x_n Z_n$, and an addition followed by $(m-1)m^L$ binary comparisons.

Both memory and computation requirements are exponentially increasing with the channel constraint length L, just as in the original VA used in Forney's structure. However, in consideration of computation, this modified VA has some advantage over the original VA because here only multiplication, addition and comparisons are required to be done in real time. The original VA requires subtraction, squaring, addition, and comparisons in real time. In other words, a multiplication operation replaces both subtraction and squaring.

3.4 Performance of the Receiver

Ungerboeck [4] provided a performance analysis of the receiver in a way similar to Forney [5], showing that the same probability of error applies to both receiver structures.

The error sequence and error event concepts will be used in deriving the probability of error. We define error sequence as the difference between an estimated sequence and the actual input sequence.

$$\{e_n\} \triangleq \{\hat{x}_n\} - \{x_n\} \tag{3.18}$$

An error event is defined as an error sequence extended from time 0 to H.

$$\varepsilon : \{e_n\} = \text{---}\ 0,\ 0,\ e_o,\ e_1,\ \text{---}\ e_H,\ 0,\ 0,\ \text{---} \tag{3.19}$$

where $|e_o|$ and $|e_H| > 0$, $H \geq 0$.

Define E as the set of all error events permitted by the coding rule. Using the union bound [19], we have that the probability that any error event occurs is upper bounded by

$$P_r(E) \leq \sum_{\varepsilon \epsilon E} P_r(\varepsilon) \tag{3.20}$$

To compute the probability of an error event, we observe that for a distinct error event ε to happen, two sub-events ε_1 and ε_2 must occur [4].

ε_1 : $\{\hat{x}_n\}$ is such that $\{x_n\} + \{e_n\}$ is also an allowable input sequence.

ε_2 : the noise terms are such that $\{\hat{x}_n\} + \{e_n\}$ has greater likelihood than $\{\hat{x}_n\}$

Accordingly

$$P_r(\varepsilon) = P_r(\varepsilon_1)\, P_r(\varepsilon_2/\varepsilon_1) \tag{3.21}$$

where the conditional probability is

$$P_r(\varepsilon_2/\varepsilon_1) = Q[\sqrt{(S/N)\delta^2(\varepsilon)/2}] \tag{3.22}$$

The error function is defined as

$$Q(x) \triangleq \frac{1}{\sqrt{2\pi}} \int_x^\infty \exp\,(-y^2/2)\, dy \tag{3.23}$$

and the SNR is

$$S/N \triangleq s_o/N_o \tag{3.24}$$

where N_o is one-sided noise spectral density.

$\delta^2(\varepsilon)$ is the square distance between any two different transmitting sequences normalized by the PRS system energy. $\delta^2(\varepsilon)$ can also be considered as the energy of the signal that results from passing the error sequence ε through the PRS filter.

$$\delta^2\,(\varepsilon) \triangleq \frac{1}{s_o} \sum_{i=0}^{H} \sum_{k=0}^{H} e_i\, s_{i-k}\, e_k$$

$$= d^2(\varepsilon)/s_o \tag{3.25}$$

Therefore, the error function can be rewritten as

$$Q\sqrt{(S/N)\delta^2(\varepsilon)/2} = Q\left[\sqrt{\frac{s_o}{N_o}\cdot\frac{d^2(\varepsilon)}{s_o}/2}\,\right]$$

$$= Q[d(\varepsilon)/2\sqrt{N_o}]$$

$$= Q[d(\varepsilon)/2\sigma] \qquad (3.26)$$

where σ^2 is the noise variance.

Equation (3.21) becomes

$$P_r(\varepsilon) = Q[d(\varepsilon)/2\sigma]\; P_r(\varepsilon_1) \qquad (3.27)$$

Accordingly

$$P_r(E) \leq \sum_{\varepsilon\varepsilon E} Q(d(\varepsilon)/2\sigma)\; P_r(\varepsilon_1)$$

$$\leq \sum_{d\varepsilon D} Q(d/2\sigma) \sum_{\varepsilon\varepsilon E_d} P_r(\varepsilon_1) \qquad (3.28)$$

where D is the set of all allowable distances $d(\varepsilon)$, and E_d is the subset of all error events for which $d(\varepsilon) = d$.

At moderate SNR, $P_r(E)$ will be dominated by the term involving the minimum value of $d(\varepsilon)$ because $Q(x)$ is an exponentially decreasing function [4]. We have

$$P_r(E) \doteq Q(d_{min}/2\sigma)\cdot K_1$$

where $K_1 = \sum_{\varepsilon\,\varepsilon\,E_{d_{min}}} P_r(\varepsilon_1)$

and K_1 only depends on the coding scheme.

The minimum square distance is defined as

$$d^2_{min} \triangleq \min_{\varepsilon} \{ \sum_{i=0}^{H} \sum_{k=0}^{H} e_i \, s_{i-k} \, e_k \} \quad . \tag{3.30}$$

The free distance d^2_{free} is $\min_{H} d^2_{min}$. This probability of error is the same as that of Forney's receiver [5].

The probability of symbol error can be found by weighting each error event by the number of decision errors. It was shown [13] that the probability of symbol error is upper bounded.

$$\begin{aligned} P(e) &\leq \sum_{\varepsilon\epsilon E} W_H(\varepsilon) \, P(\varepsilon \;) \\ &\leq \sum_{\varepsilon\epsilon E} W_H(\varepsilon) \, P_r(\varepsilon_1) \sum_{d\epsilon D} Q(d/2\sigma) \\ &= K_2 Q(d_{free}/2\sigma) \end{aligned} \tag{3.31}$$

where $\quad K_2 = \sum_{\varepsilon\epsilon E_{d_{free}}} W_H(\varepsilon) \, P_r(\varepsilon_1)$ and

$W_H(\varepsilon)$ is the Hamming distance of the error event ε.

3.5 Some Discussion

In the above sections, we have already shown that Ungerboeck's receiver is another nonlinear receiver implementing MLSE besides Forney's receiver. Both receivers have the same error performance.

However, we feel that Ungerboeck's receiver is more realistic because no whitening filter is required. In Forney's receiver, the statistical independence of noise samples at the output of the matched filter is essential and hence a whitening filter with transfer function $1/F(\omega)$ [5], must follow the matched filter to decorrelate the noise. It is obvious that the whitening filter will become unstable if the transmitting filter $F(\omega)$ has some zeroes located outside the unit circle in the Z-plane. This will cause the receiver to collapse. From this point of view, a receiver without use of a whitening filter is necessary condition in many channels, for instance multipath channels.

Moreover, in terms of computation, Ungerboeck's receiver is a little more efficient than Forney's receiver because no squaring and subtraction are required but only multiplication.

We have shown that complexity of this kind of receiver is exponentially increasing as the channel length. Therefore, it can only be practically applied to a short channel length. However, the complexity brings a reward of better performance. Wong [13] has shown the performance of MLSE receiver is better than a receiver based on decision feedback equalization in both probability of symbol error and SNR. Conventional equalization methods apply a linear filter to eliminate the effect of ISI and it is inevitable that the noise is enhanced. An MLSE receiver eliminates ISI without increasing noise because it exploits the discreteness of the ISI and it makes a decision on the sequence rather than symbol by symbol as in the equalization receiver. A more detailed analysis of zero forcing equalization and decision feedback equalization was presented by Messerschmitt [31] using a geometric approach. This is reviewed in Wong [13].

CHAPTER 4

COMPUTATION OF MINIMUM DISTANCE - d_{free}

The minimum distance d_{free} is a fundamental performance parameter of maximum likehood sequence estimation. The properties of minimum distance d_{free} and an algorithm for computation of d^2_{free} are presented.

4.1 Representation of d^2_{free}

The minimum square distance d^2_{free} can be represented in quadratic form [4].

$$d^2_{free} \triangleq \min_{\varepsilon} \left\{ \sum_{i=0}^{H} \sum_{j=0}^{H} e_i \, s_{i-j} \, e_j \right\} \tag{4.1}$$

where H is the length of an error event E

S_ℓ is the pulse autocorrelation sequence

For a given PRS scheme, the autocorrelation sequence s_ℓ is known and fixed, so the determination of d^2_{free} depends on the selection of error event E. To find d^2_{free}, one can search overall allowable error sequences to find the specific sequence that associates with d^2_{free}.

Another representation of d^2_{free} is given from signal space concepts [17]. We can consider d^2_{free} as the minimum square distance between any two sequences among all possible transmitting sequences. Since a PRS system can be represented by a shift register (a finite state machine), all the transmission sequences can be completely represented by a tree or trellis. One should keep in mind that the group property of a binary convolutional encoder does not hold for a PRS system even though it is a real number convolutional encoder. The operation is in the real number field with reducdancy introduced amplitudewise. The mathematical representation of the above defined d^2_{free} is [13].

$$d^2_{free} \triangleq \min_i \min_j [\|Y_i(D)-Y_j(D)\|^2 \text{ for each } j \neq i,\ 1 \leq j \leq m^N]$$

$$\text{for each } 1 \leq i \leq m^N,\ K \leq N \leq \infty\} \qquad (4.2)$$

where $\|Y_i(D) - Y_j(D)\|^2 = \sum_{k=1}^{N} (Y_{ik}-Y_{jk})^2$

One straightforward approach to find d^2_{free} by (4.2) is the so-called brute force method that computes all the possible codewords and then compares the distances among those codewords to choose the minimum square distance. However, this method can never be used in practice because of the large number of possible codeword pairs equal to $(m-1)\ (2m-1)^{N-1}$. The computation and memory are exponetically increasing with N, so only a very small value of N and m may be dealt with by the brute force method.

Wong proposed [13] a method called double dynamic programming that is more efficient than the brute force method. However, the memory requirement and computational time are still exponentially increasing with the channel constraint length (though not with N). As a result, it is only suitable for channels with short constraint length.

4.2 Properties of d^2_{free}

Some important properties of d^2_{free} will be mentioned and used for deriving an algorithm to compute d^2_{free} in a more efficient way.

From (4.2), we observe that d^2_{free} has the additive property, which means the distance is accumulated at each symbol interval and increases along with symbol time. The additive property induces another fact that d^2_{free} is upper bounded. Whenever a distance is found for one sequence pair, d^2_{free} is upper bounded by the found distance. Hence, if any distance due to other pairs of codewords exceeds such an upper bound, it will not be the d^2_{free} and can be discarded.

When we view d^2_{free} by the error event space concept as in (4.1), d^2_{free} of a fixed PRS system depends only on error event $\{e_0, e_1, \ldots e_H\}$. For binary input data {0, 1}, the error sequence can only be a sequence containing 0,1 or -1. When a pair of codewords at time t expands to time t+1, there will be four new pairs of codewords as shown in Fig. 4.1. Therefore the four possible error signals e are as below.

			1	2	3	4
Pair of codewords	Transmitting sequence =	T	0,	0,	1,	1
	Neighbour sequence =	N	0,	1,	0,	1
	Error sequence =	e	0,	-1,	1,	0

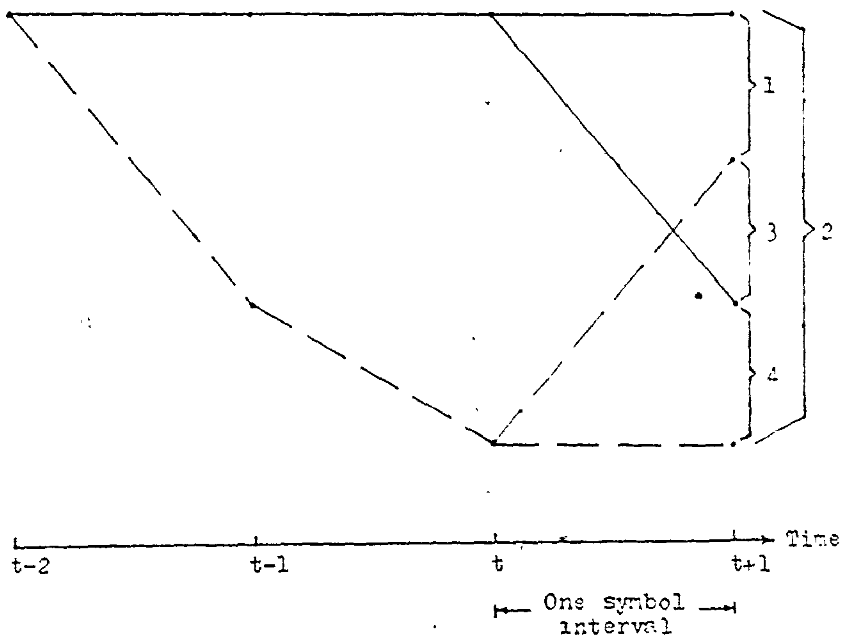

Fig. 4.1 Expansion of a pair of codewords at t. Assuming channel constraint length is equal to three.

We observe that two error sequence elements e are the same (0), so we only need consider one of them. As a result, when we search for d^2_{free} along a trellis diagram, for each pair of codewords at time t expanding to time t+1, we need consider only three of the four new grown pairs of codewords.

4.3 An Algorithm for Computation of d^2_{free}

A fast sequential algorithm was introduced by Aulin and Sundberg [18] for computation of the minimum distance of M-ary correlative encoded continuous phase frequency shift keying with a MLSE receiver. The algorithm is based on the facts that the minimum distance is additive and upper bounded. A phase tree was developed for computing minimum distance which is a function of the modulation index h.

Using the same concept, we have developed an algorithm to compute the minimum square distance d^2_{free} of a correlative encoder with MLSE receiver. This algorithm is similar to a stack algorithm proposed for sequential decoding [19], which is based on "metric first" searching of a tree. In this type of search, new searching occurs only in front of the node most likely to lead to the best outcome.

The modified stack algorithm for computation of d^2_{free} is an algorithm to search on a state trellis diagram for all possible potential codeword pairs that may cause d^2_{free}. Applying the incremental and upper bounded properties of d^2_{free} in signal space, we can limit the number of possible potential codewords into a manageable size.

First, an initial upper bound of d^2_{free}, called d^2_B, must be provided. We do not have any idea of the possible value of d^2_{free} of a channel code at the beginning, but we can assume as an upper bound an allowable error sequence that caused a distance. The error event ε = 1-D is chosen to initialize the upper bound. Thus we have

$$\text{Initial } d_B^{\,2} = \sum_{i=0}^{1} \sum_{j=0}^{1} e_i \, s_{i-j} \, e_j$$

$$= e_0^{\,2} s_0 + e_1^{\,2} s_0 + e_0 e_1 s_{-1} + e_1 e_0 s_1$$

$$= (e_0^{\,2} + e_1^{\,2}) s_0 + e_0 e_1 s_1 \qquad \text{since } s_\ell = s_{-\ell}$$

$$= 2s_0 - 2s_1 \qquad \text{since } e_0 = 1,\ e_1 = -1$$

$$= 2\,(s_0 - s_1) \tag{4.3}$$

Three stacks are required for implementing our algorithm. Two stacks, called TS and NS are used for storing all possible pairs of sequences that have square distances not exceeding the upper bound $d_B^{\,2}$. The corresponding distance is stored in a third stack called DS. Each word in the TS and NS stacks represents one sequence. Since a sequence can only contain a binary number {0, 1} for binary input data, each bit of a word in TS and NS is then used to represent one symbol of a sequence. The algorithm is implemented on a CDC 6400 computer, in which each word has 60 bits, so one word can store a sequence with a maximum 60 symbols.

Consider searching on the trellis diagram. Assuming the first symbol of all possible error sequence is one, at the first symbol time interval we can only have one pair of sequences. We proceed to next symbol interval, and one pair of sequences will expand to three new pairs of sequences (two of the four pairs of sequences have the same error and will result in same distance, so only three pairs are needed to be considered). Those expanded new sequence pairs are stored in the two stacks TS and NS if their distances are less than ${d_B}^2 - f^2_{k-1}$, otherwise they are discarded. We can discard the sequence pairs with distance greater than ${d_B}^2 - f^2_{k-1}$ rather than ${d_B}^2$, because we observe that the final increment to d^2_{free} that occurs just before a merge is always equal to f_{k-1}; i.e.,

$$(Y_{iN} - Y_{jN})^2 = f^2_{k-1} \tag{4.4}$$

where two sequences merge at stage N.

This can be explained by the states of two sequences that can only be different in their final symbol just before merging into the same state. Therefore the distance contributed at this stage can only derive from the last tap coefficient f_{k-1}. From (4.2), d^2_{free} is the cumulated distance of two diverged sequences. So whenever a non-merged sequence pair has a distance greater than ${d_B}^2 - f^2_{k-1}$, it can never lead to d^2_{free}. All the sequences stored in TS and NS must satisfy the following conditions

(i) All are unmerged sequences

(ii) $d_i^{\ 2} \leq d_B^{\ 2} - f_{k-1}^2$ (4.5)

where d_i is the unmerged distance of the sequences pair.

All the merged-sequence distances will be compared with $d_B^{\ 2}$. If the merged-sequence distance is smaller than $d_B^{\ 2}$, it updates the value of $d_B^{\ 2}$,and tightens the upper bound.

When the TS and NS stacks have more than one sequence, we will select the pair for expansion with the smallest distance. If the merged distance is smaller than the smallest distance stored in the stack, then we can claim that the merged distance is d_{free}^2 as well. Otherwise, we will expand the selected smallest distance sequence pair and repeat the comparison procedure as mentioned above.

The logical flowchart of the program is shown in Fig. 4.2.

4.4 Complexity and Efficiency of the Modified Stack Algorithm

The algorithm presented in last section has successfully computed the minimum square distance d_{free}^2 for channel lengths up to twelve. The efficiency of the algorithm depends on the following facts.

First the tightness of upper bound $d_B^{\ 2}$. The number of possible pairs sequences that may cause $d^2_{\ free}$ greatly depends on $d_B^{\ 2}$. If a tight upper bound is set, the algorithm finds $d^2_{\ free}$ much faster. In our simulation, the initial upper bound is set up by considering the error event 1-D that causes $d_B^{\ 2}$. In general

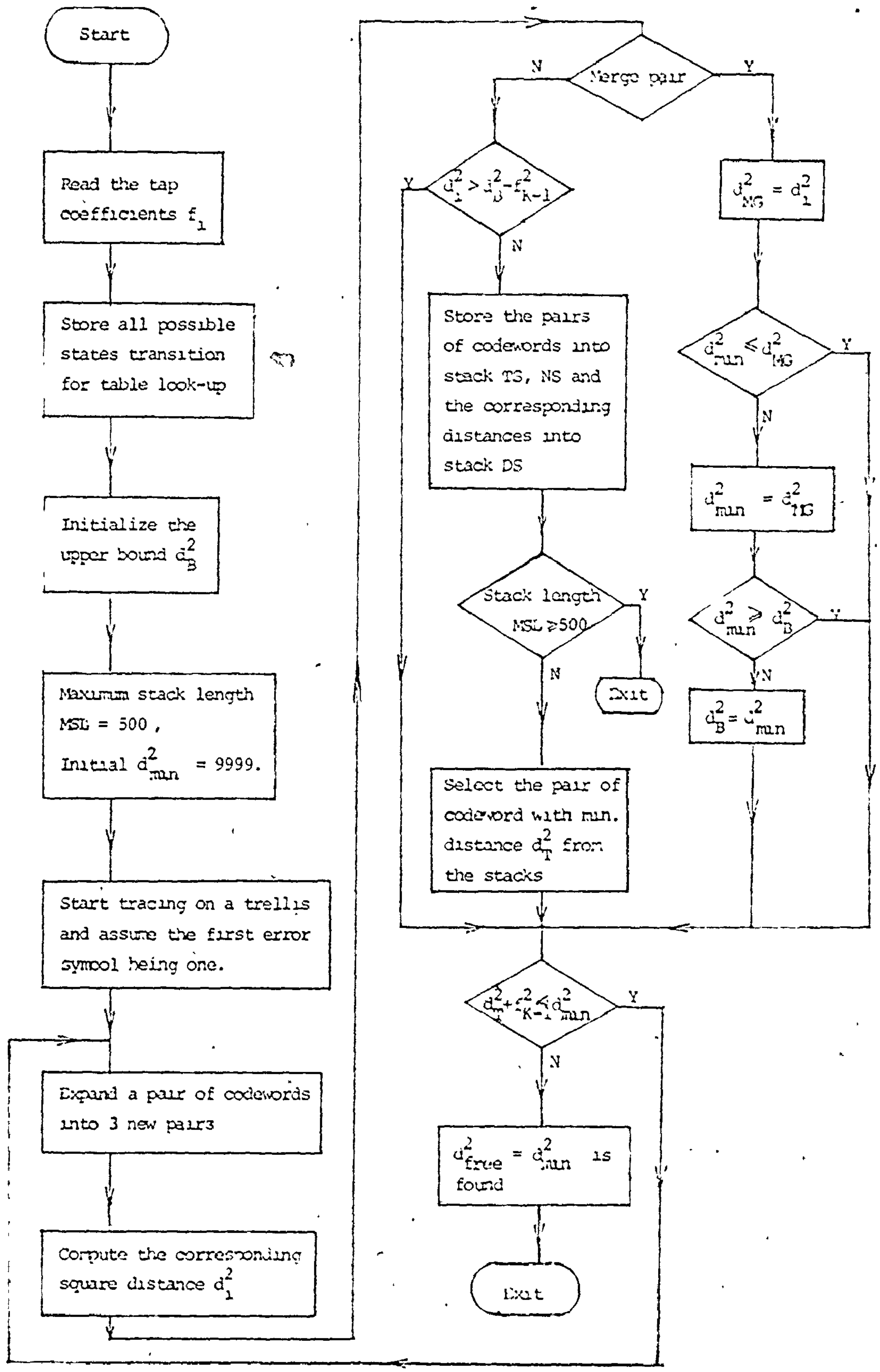

Fig. 4.2 Flowchart of the modified stack algorithm

this initial upper bound is quite tight, especially for channel lengths less than eight, because the error sequence 1-D is the error sequence that causes d^2_{free} for a short channel length. If the initial guessed upper bound is not a tight one, $d_B{}^2$ can still get tighter during the search. However, the speed of convergence to d^2_{free} will be slower than that of a good initial guessed upper bound.

The second important factor that affects the efficiency of our algorithm, is the characteristics of the channel code. If a channel code has a very long decision depth which is defined [13] as the least depth in a trellis at which all pairs of sequences, either merged or not, have Euclidean distance between them greater than the free distance d^2_{free}, the algorithm will require more memory locations and computational time to get the d^2_{free}. We have to trace on the trellis for more symbol intervals. There are some channels that can cause catastrophic error propagation, which means decision depth is infinite. Wong [13] presented some specific examples and described the nature of these codes. For these, we have to decide the minimum merged distance in a finite symbol intervals eventhough there are still some nonmerged pairs of sequences with smaller Euclidean distance. Of course, these codes will not achieve the performance predicted by the free distance for any finite decoder memory. In our work, we take a maximum of sixty symbol intervals; after that a guess at d^2_{free} has to be made.

Memory requirement and computational time are used to count the complexity of the algorithm.

The memory requirement of this algorithm depends on the size of the three stacks that are used to store pairs of sequences and corresponding distances. Since the number of possible pairs of sequences is different for different channel codes, no fixed memory requirement of the three stacks can be presented for different channel lengths. However, through the simulation we observe that in general a stack with 200 memory locations is enough for most codes with channel length less than twelve. In order to provide a larger margin, we set stack length equal to five hundred. Therefore the memory required for the three stacks is $3 \cdot (500) = 1500$ memory locations. On the whole, the stack length increases as the channel length increases because a longer channel length will cause a longer decision depth and so more possible pairs of sequences.

The memory requirement is much less than that of the double dynamic programming. The memory required for the double dynamic programming is exponentially increasing as the channel length. It was shown [13] that $2 \cdot (m^{2L})$ memory locations are necessary and some more memory may be required for tracing the pairs of sequences. In general, the double dynamic programming method is only suitable for a shorter channel.

The computational time required for executing the algorithm depends on the channel characteristic as well. In general the computational time is proportional to the channel length provided the code is non-catastrophic and the initial upper bound d_B^2 is good. Experience indicates that usually less than two sec CP execution time is required for computation of d^2_{free} with the channel length less than twelve. In comparison, with the double dynamic programming method the computation time is exponentially increasing as the channel length. For instance, about 60 sec CP execution time is used for a code with channel length equal to seven. The same code computed by the modified stack algorithm only needs less than one sec. For a shorter channel length (K less than five), the two algorithms do not show much difference in computation time, but in a longer channel length the modified stack algorithm will be much more efficient than the double dynamic programming method. Especially when we handle the optimization problems that will be discussed in Chapter 5 to 8, we need compute d^2_{free} many times in searching an optimal solution and the efficiency in computation of d^2_{free} is extremely important for success in solving the optimization problems.

CHAPTER 5

OPTIMIZATION TECHNIQUES

This chapter introduces an optimization technique called nonlinear programming (NLP) and a computer package Flopt 5 that was designed for solving different kinds of optimization problems. The analogy between the nonlinear programming problem and the minimax problem is also discussed.

5.1 Problem Statement

An optimization problem is usually a problem to find a minimum or maximum of an objective function subject to equality and/or inequality constraints. The constraints can be linear and/or nonlinear. This kind of optimization problem is the so-called constrained NLP problem [20]. It can be formulated as following

$$\text{Min} \quad U(\underline{x}) \tag{5.1}$$

subject to m inequality constraints $g_i(\underline{x}) \geq 0 \quad i=1,2,\ldots m$

ℓ equality constraints $h_j(\underline{x}) = 0 \quad j=1,2,\ldots \ell$

where $\underline{x}$ is a vector of K independent variables.

In a design problem, $\underline{x}$ may be the design parameters and the objective function $U(\underline{x})$ may be a cost function. The constraints $g_i(\underline{x})$ and $h_j(\underline{x})$ can be the specifications.

There are various methods for solving the above optimization problem. Basically, it can be divided into two classes.

(a) Analytical Approach

The fundamental tools of this method are differential calculus and variational calculus. When the problem has inequality constraints, Lagrange multiplier and constrained variation are the basic techniques to solve the problem [21]. In order to apply this technique, the mathematical terms in the problem must be manipulated by certain available rules. The advantage of this classical method is that an exact solution can be found in closed form. However, in many problems that may consist of highly nonlinear functions, it may be impossible to find a solution analytically.

(b) Numerical Approach

The numerical approach is to solve the optimization problem by means of some efficient iterative procedures. A careful formulation of the problem and the iteration procedure can generate a solution as accurate as that by an analytical method. There are many different algorithms available for solving the NLP problem [20]. Usually these algorithms consist of the formulation of an objective function, a routine to search the minimum value of the objective function by gradient search methods or other efficient searching algorithms. We will use this approach to solve our optimization problems later on.

5.2 The Kuhn-Tucker Conditions

The necessary conditions for optimal solution of a NLP problem defined by (5.1) were derived by Kuhn and Tucker [22] and known as Kuhn-Tucker conditions.

The Kuhn-Tucker conditions state that the necessary conditions for a point $\underline{x}$ to be a local minimum (or maximum) of $U(\underline{x})$ subject to $g_i(\underline{x}) \geq 0$ are

$$\nabla U(\underline{x}) = \sum_{i=1}^{m} u_i \nabla g_i(\underline{x}) \tag{5.2}$$

and

$$\underline{u}^T \underline{g}(\underline{x}) = 0 \tag{5.3}$$

where $\underline{u} \triangleq \begin{bmatrix} u_1 \\ \vdots \\ u_m \end{bmatrix} \geq 0$ are called Kuhn-Tucker multipliers.

$$\underline{g}(\underline{x}) \triangleq \begin{bmatrix} g_1 \\ \vdots \\ g_m \end{bmatrix}$$

$$\nabla U(\underline{x}) \triangleq \begin{bmatrix} \frac{\partial U}{\partial x_1} \\ \vdots \\ \frac{\partial U}{\partial x_k} \end{bmatrix} \qquad \nabla g_i(\underline{x}) \triangleq \begin{bmatrix} \frac{\partial g_i}{\partial x_i} \\ \vdots \\ \frac{\partial g_i}{\partial x_k} \end{bmatrix}$$

Under convex programming [20], which means $U(\underline{x})$ is convex and $g_i(\underline{x})$ is concave and the feasible region is nonempty, then the necessary conditions will become sufficient for $\underline{x}$ to be an optimal solution. In practical problems, the sufficient conditions are quite restrictive but if we have been using a reliable optimization method and if the relations are satisfied, we can be reasonably sure that a local minimum has been attained even if the convexity requirement is not met [23].

5.3 Techniques to Solve the Constrained Problem

It is usually easier to solve an unconstrained NLP problem than a constrained NLP problem. Therefore, a constrained problem is usually converted into an unconstrained problem. There are several techniques for reformulating a constrained optimization problem.

A method which has been widely used is the penalty method. It transforms the objective function of a constrained minimization problem by some functions of the constraints and the constrained minimum is obtained as the limit of a sequence of unconstrained minima of the modified objective function. Various penalty functions for inequalities and/or equalities have been proposed and the most relevant are due to McCormick [24], Fletcher [25]. The main drawback of applying penalty functions is that ill-conditioning will happen as the control parameters of the penalty function tend to zero or infinity.

Bandler and Charalambous [26] suggested to transform a constrained optimization problem into an unconstrained minimax problem. "The original NLP problem is formulated as an unconstrained minimax problem. Under reasonable restrictions, it is shown that a point satisfying the necessary conditions for a minimax optimum also satisfies the Kuhn-Tucker necessary conditions for the original problem." pp. 627, [26].

The transformation of a NLP problem into an unconstrained minimax problem is shown below.

NLP Problem: $\text{Min } U(\underline{x})$

subject to $g_i(\underline{x}) \geq 0$, $i=1, \ldots, m$.

Unconstrained Minimax Problem: $$\text{Min}\{V(\underline{x},\underline{\gamma}) = \max_{1\leq i\leq m}[U(\underline{x}),\ U(\underline{x}) - \gamma_i g\ (x)]\} \qquad (5.4)$$

where $\gamma_i > 0$, $i=1, \ldots m$, γ_i is similar to a weighting function,

and $\underline{\gamma} = [\gamma_1, \gamma_2, \ldots \gamma_m]^T$.

It has been shown [26] that the condition for optimality of the minimax objective function $V(\underline{x},\underline{\gamma})$ with respect to $\underline{x}$ is that,

$$\sum_{i=1}^{m} (u_i/\gamma_i) < 1 \qquad (5.5)$$

where u_i are the Kuhn-Tucker multipliers.

So it is important to choose γ_i large enough such that (5.5) is satisfied, otherwise the optimal point may be selected in the nonfeasible region.

Bandler and Charalambous [26] pointed out that the minimax objective function $V(\underline{x},\underline{\gamma})$ will have discontinuous first partial derivatives at points where two or more of the function (5.4) are equal to $V(\underline{x},\underline{\gamma})$. This disadvantage can be removed by smoothing the function at the points at which the function is not differentiable. This can be done by introducing the generalized least pth objective function [27], which is a pth norm-like function. The minimax solution will be approximated as p approaches infinity. An accelerated least pth algorithm for minimax optimization was developed by Charalambous [28], which approaches the minimax solution much faster and overcomes the ill-conditioning when approaching the minimax solution.

The overall procedure for solving a constrained optimization problem by the minimax techniques and least pth approximation is shown in Fig. (5.1). This technique will be applied to our constrained problems in Chapter 7 and 8.

The unconstrained minimization of the least pth objective function can be done by any efficient unconstrained minimization algorithm. Various methods that work with or without employing gradient information are available [23]. An algorithm proposed by Fletcher [29] is used here, which applies gradient vectors to estimate the search direction.

5.4 A Computer Package Flopt 5

An optimization program called Flopt 5 was designed by

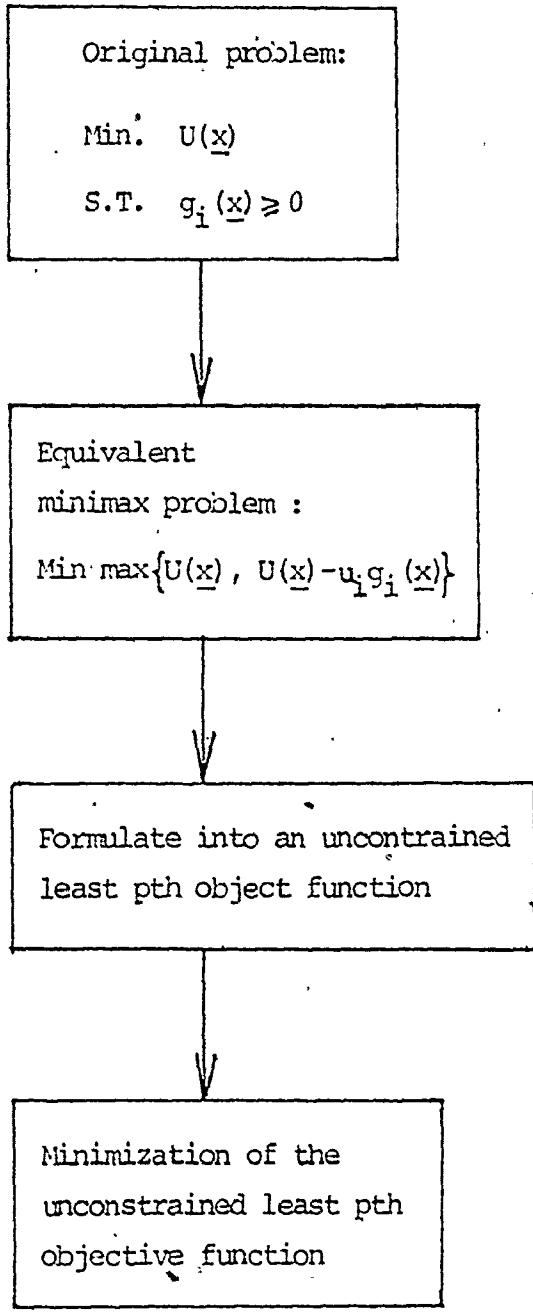

Fig. 5.1 An approach to solve a contrained NLP problem, where S.T. means subject to.

Bandler and Sinha [30]. It is a program designed for minimax optimization using the accelerated least pth algorithm. Optimization problems ranging from unconstrained to constrained problems can be solved by Flopt 5.

Flopt 5 is a package of subroutines and three of the most important subroutines are

-- FLOPT 5 which executes the accelerated least pth algorithm.

-- LEASTP5 which formulates the least pth objective function.

-- QUASI 5 which performs unconstrained minimization using Fletcher algorithm.

In order to use this package, the user has to provide a main program and a subroutine called Funct 5. The main program provides initial values of certain variables and calls subroutine Flopt 5. The subroutine Funct 5 is used to define the problem to be solved and provides the gradient functions.

5.5 Application to Our Work

Flopt 5 will be applied to solve our optimization problems in the following Chapters, including one unconstrained problem and two constrained problems.

First, minimization of d^2_{norm}.

Second, minimization of bandwidth with the 99% energy bandwidth constraint.

Third, minimization of bandwidth with the 99% energy bandwidth constraint and ISI degradation constraint.

CHAPTER 6

MINIMUM FREE DISTANCES OF PRS SYSTEMS WITH CHANNEL LENGTHS UP TO TWELVE

In Chapter 4, we showed that the free distance of a real number convolutional code can be found by the modified stack algorithm. A computer package Flopt 5 was introduced in the last chapter for solving several kinds of optimization problems. This chapter will apply the modified stack algorithm and Flopt 5 to find the worst possible performance of a PRS system with a ML receiver for channel lengths up to twelve. The pulse shaping filter is an ideal low pass filter of width 1/2T Hz.

6.1 Normalized d^2_{free} and Degradation

The minimum square distance d^2_{free} has been defined as

$$d^2_{free} \triangleq \min_{\varepsilon} \{ \sum_{i=0}^{H} \sum_{j=0}^{H} e_i \, s_{i-j} \, e_j \} \tag{6.1}$$

If we scale up the tap coefficients, the minimum square distance d^2_{free} will be increased accordingly. This also increases the power of the PRS system. Therefore, we may change d^2_{free} to any value we wish by scaling the tap coefficients f_i, at the expense of more transmitter power. In order to give a fair comparison between a

PRS system with different sets of tap coefficients or with different channel constraint lengths, we have to normalize the minimum square distance d^2_{free} by the output variance of the PRS filter.

Hence, a normalized d^2_{free} is defined as [13]

$$d^2_{norm} \triangleq d^2_{free}/\sigma_y{}^2 \tag{6.2}$$

$$= d^2_{free}/\sigma_x^2 R(o) \tag{6.3}$$

where R(0) is the energy of the PRS system.

$\sigma_x{}^2$ is input variance of the m-ary input data and is defined as [13]

$$\sigma_x{}^2 \triangleq (m^2-1)/12 \ . \tag{6.4}$$

The degradation of a PRS system in comparison with a single pulse PAM system can be defined as

$$\text{Degradation (DB)} \triangleq 10 \log_{10} (d^2_{norm} \text{ of PRS}/d^2_{norm} \text{ of PAM})$$

$$= 10 \log_{10} (d^2_{free}/R(0))$$

since d^2_{norm} of PAM $= 1/\sigma_x{}^2$.

Whenever we mention the degradation, we mean that the degradation in dB of a PRS system caused by ISI with respect to a single pulse PAM system. For BPSK (m=2), the d^2_{norm} is equal to 4 in our convention. Thus, when a binary system has a normalized minimum square distance d^2_{norm} equal to 4, it means no degradation in this system caused by ISI. If the d^2_{norm} is less than 4, for instance $d^2_{norm}=2$, it means the binary system will lose 3 dB in performance compared with BPSK.

6.2 Computation of the Worst Possible Degradation

It is desirable to know the worst possible degradation that can happen in a channel with a fixed constraint length. The problem can be formulated as an unconstrained optimization problem.

The problem statement is to maximize the absolute value of degradation (DB) for a fixed channel length.

$$
\begin{aligned}
\max_{f_i} (DB) &\equiv \max_{f_i} |\{10 \log_{10} d^2_{free}/R(0)\}| \\
&\equiv \min_{f_i} (d^2_{free}/R(0)) \qquad \text{since } \log_{10} (d^2_{free}/R(0)) \leq 1 \\
&\equiv \min_{f_i} (d^2_{norm} (\sigma_x^2)) \\
&\equiv \min_{f_i} (d^2_{norm}) \qquad (6.5)
\end{aligned}
$$

since $\sigma_x{}^2$ is independent of f_i.

Therefore, finding the worst possible DB is equivalent to finding the minimum d^2_{norm} over the tap coefficients space. The computation of d^2_{norm} can be done by using the modified stack algorithm while the minimization of d^2_{norm} over f_i can be done by applying the optimization package Flopt 5. The overall organization of computing $\min_{f_i} (d^2_{norm})$ is shown in Fig. 6.1. The gradient vector of d^2_{norm} is

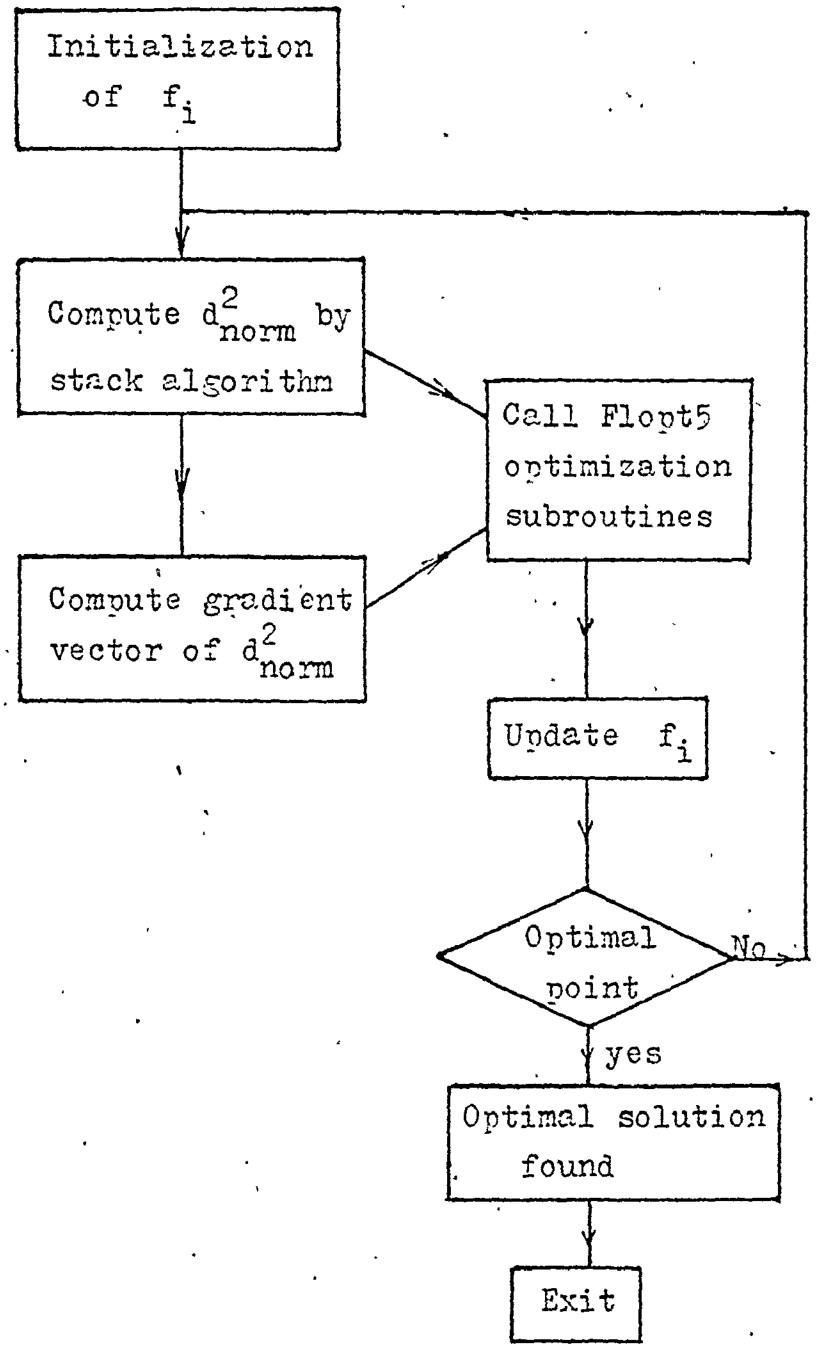

Fig. 6.1 Overall procedure for compution of minimum d^2_{norm}

$$\nabla d^2_{norm} = \frac{\partial}{\partial f_i} (d^2_{norm}) \qquad i=1,2,\ldots,K-1$$

$$= \frac{\partial}{\partial f_i} (d^2_{free}/R(0)) \qquad (6.6)$$

For a PRS system with a rectangular function as a pulse shaping filter, the energy of the PRS system is

$$R(0) = \sum_{j=0}^{K-1} f_j^{\,2} . \qquad (6.7)$$

d^2_{free} was defined in (4.2), which indicates that as soon as we found d^2_{free}, we know which two output sequences Y(D) cause the d^2_{free}. Since Y(D) is a deterministic function of f_i, we can compute the partial derivative of d^2_{free} analytically in terms of the f_i. Similarly, the partial derivatives of R(0) can also be found to be $2f_j$. Therefore, the partial derivative of d^2_{norm} in (6.6) can be represented in closed form as soon as d^2_{free} has been found.

It should be pointed out that the derivatives of d^2_{norm} may not be continuous in the whole tap coefficients space. From Wong's contour maps [13], we find there are points that have discontinuous derivatives. Fortunately, the number of discontinuous points is very small and will not affect the use of the gradient method in our optimization problem. Even if the discontinuous partial derivatives point is hit during the minimization procedure, we can change to another starting point and restart the minimization procedure. However, this condition has never happened in our computation of the worst degradation.

The results of the worst degradation for channel lengths up to twelve are shown in Table 6.1 and the corresponding curve is shown in Fig. 6.2.

6.3 Analysis of the Results

From Table 6.1, we observe that no degradation for channel lengths less than or equal to two when MLSE receiver is employed. For channel lengths between three and six, the worst degradations are caused by the same error event $\varepsilon = 1-D$. However, when the channel lengths are greater than six, the error event $\varepsilon = 1-D-D^2+D^3+D^4-D^5$ will cause the worst degradation. This is indicated by the degradation curve in Fig. 6.2, where there is a sharp change of degradation from the transition of K=6 to K=7. These results confirm the results of Magee [9] for channel lengths less than seven. Anderson [12] provided a result for K=7 only, which is also the same as ours.

Another interesting property of the worst-case channel codes is that the tap coefficients are symmetry about the central tap coefficient, i.e. $f_i = f_{K-i}$, $0 \leq i \leq K$. Although no proof for this property is available for channel lengths greater than twelve, it is reasonable to assume that this property will still hold for other channel lengths. Hence we can reduce the number of variables f_i of the optimization problem from K-1 (since we assume $f_0=1$) to $[\frac{K-1}{2}]$. The reduction in the number of variables will make the optimization procedure converge to the optimal point faster. Therefore, when we

K	DB	The worst degradation channel codes F(D)	Error event
2	0.	$1+D$	1
3	2.23	$1+1.41D+D^2$	$1-D$
4	4.18	$1+1.62D+1.62D^2+D^3$	$1-D$
5	5.72	$1+1.73D+2.00D^2+1.73D^3+D^4$	$1-D$
6	7.03	$1+1.80D+2.25D^2+2.25D^3+1.80D^4+D^5$	$1-D$
7	8.84	$1+1.76D+2.66D^2+2.97D^3+2.66D^4+1.76D^5+D^6$	$1-D-D^2+D^3+D^4-D^5$
8	11.54	$1+1.54D+2.75D^2+3.12D^3+3.12D^4+2.75D^5+1.54D^6+D^7$	$1-D-D^2+D^3+D^4-D^5$
9	13.20	$1+1.94D+3.23D^2+4.26D^3+4.45D^4+4.26D^5+3.23D^6+1.94D^7+D^8$	$1-D-D^2+D^3+D^4-D^5$
10	14.69	$1+1.85D+3.48D^2+4.50D^3+5.31D^4+5.31D^5+4.50D^6+3.48D^7+1.85D^8+D^9$	$1-D-D^2+D^3+D^4-D^5$
11	15.75	$1+2.01D+3.70D^2+5.26D^3+6.22D^4+6.88D^5+6.22D^6+5.26D^7+3.70D^8+2.01D^9+D^{10}$	$1-D-D^2+D^3+D^4-D^5$
12	16.37	$1+2.18D+4.18D^2+6.09D^3+7.78D^4+8.74D^5+8.74D^6+7.78D^7+6.09D^8+4.18D^9+2.18D^{10}+D^{11}$	$1-D-D^2+D^3+D^4-D^5$

Table 6.1 The worst degradation and the corresponding channel codes.

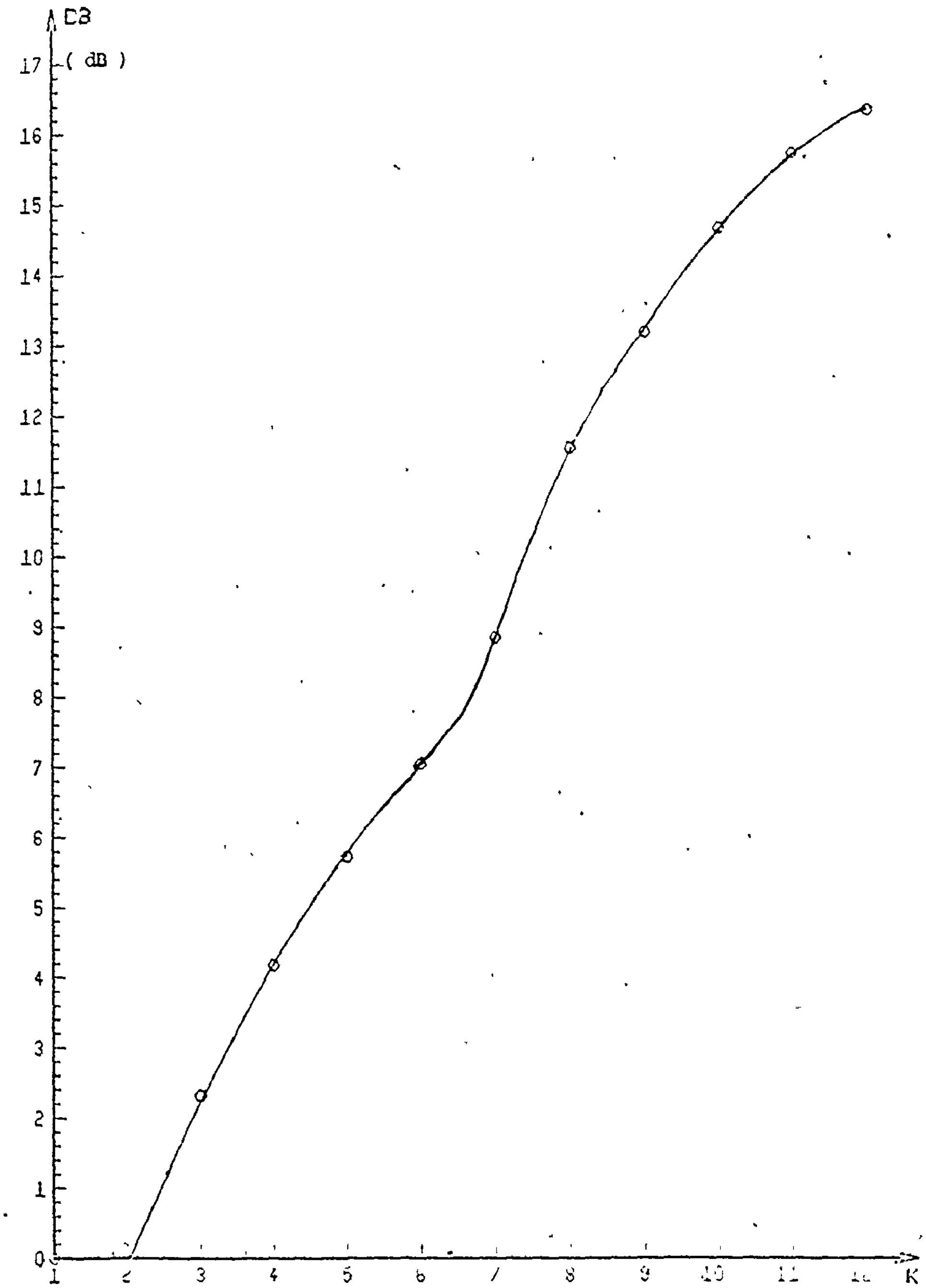

Fig. 6.2 The worst performance loss versus channel length

find the worst degradation channel code, we assume the symmetric property being true for the tap coefficients f_i and do the optimization. After we get the optimal code, this is used as the initial starting point for the optimization program but no symmetric property is assumed at this time. However, if the symmetry property is true, it will approach to the optimal solution immediately since the starting point is actually the optimal point as well. As a result, this approach can save a lot of computational time for optimization and still make sure the real optimal solution is obtained.

A PRS filter is equivalent to a finite impulse response filter (FIR), so it is desirable to know the locations of zeroes of the filter in Z-plane because it can provide some information about the energy distribution of the PRS filter. To find the zeroes of a channel code, we only need to convert F(D) into Z domain and then find the roots of the Z polynomial.

For instance, when K=3, the channel code $F(D) = 1 + 1.414D + D^2$ gives the worst degradation. The Z-transform of F(D) is

$$Z[F(D)] = 1 + 1.414Z^{-1} + Z^{-2} \qquad \text{since } D = Z^{-1}$$

$$= Z^{-2}(Z^2 + 1.414Z + 1)$$

$$= Z^{-2}[Z + (0.707-j0.707)][Z + (0.707 + j0.707)]$$

Thus, the zeroes of this code are $-0.707 \pm j0.707$. The same approach has been applied to all other worst degradation channel codes and the zeroes and their locations on the Z-plane are shown in Fig. 6.3.

We observe that the zeroes of all the worst degradation channel codes are located on the unit circle. A zero on the unit circle with an angle ω radians represents a null at frequency ω radians in the frequency spectrum. A null at frequency ω will result in pulling down the energy around ω. As the channel length K increases, the number of zeroes on the unit circle will also increase and hence more nulls will be introduced in the frequency spectrum. We also observe that the increasing number of zeroes extends from the left-hand side to the right-hand side of the unit circle as shown in Fig. 6.3. This means that the energy of the PRS filter will be further pulled down in the lower frequency region in additional to the pulling down at high frequencies as K increases. Therefore, we can expect that the bandwidth requirement decreases as K increases. This will be illustrated in Chapter 7.

Moreover, the worst degradation caused by ISI for a longer channel length is quite large even with the application of MLSE at the receiving end. For instance, when K is greater than eight, the degradation DB is larger than 10 dB.

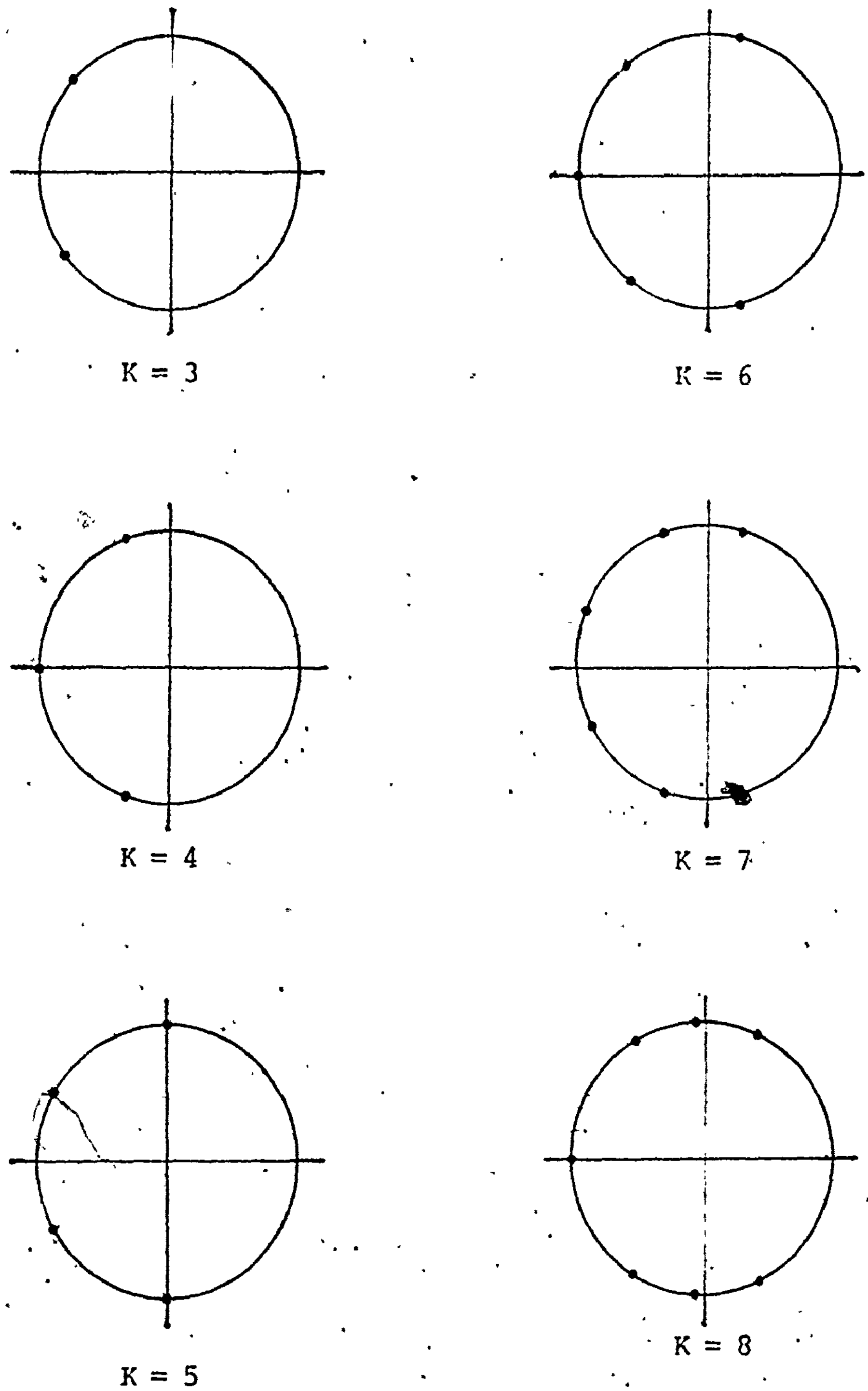

Fig. 6.3 Zero locations in the Z-plane for PRS filter with the worst degradation.

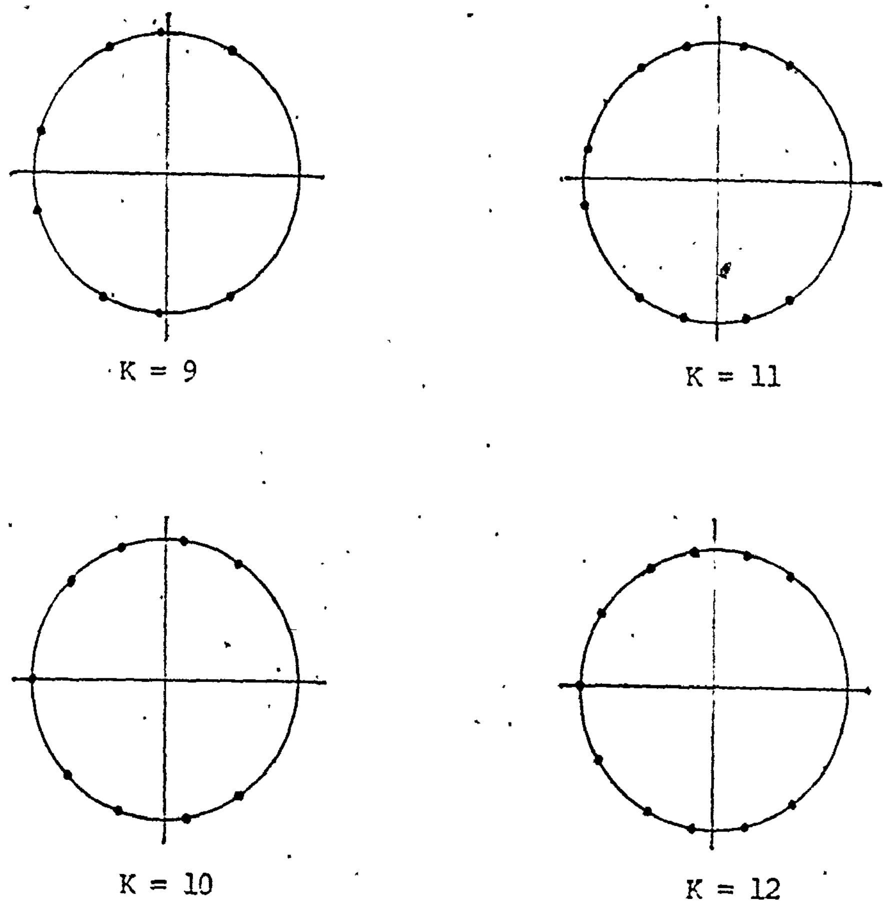

Fig. 6.3 Zero locations in the Z-plane for PRS filter with the worst degradation.

CHAPTER 7

MINIMIZATION OF BANDWIDTH WITH AND WITHOUT DEGRADATION CONSTRAINT

Bandwidth and power are the two costs in a communication system. It is desirable to have a system that requires as little bandwidth as possible while still maintaining the performance in a certain degree. However, the saving of bandwidth is usually paid for by the degradation of noise performance or by increasing the system power. For different communication channels, the importance of bandwidth and power will also be different. Therefore, the trade-off between bandwidth and power of the transmission system is worth investigating.

7.1 Definition of 99% Energy Bandwidth

The 99% energy bandwidth is usually used to measure the effective bandwidth of the transmitting system. A PRS system introduces correlation between input signals, redistributes the energy of the signal, with the result that most of the energy is located in certain frequency regions, for instance, the low frequency region. Therefore, the high frequency region contains very little energy and may be discarded with little loss of information. As a result, some bandwidth can be saved.

The 99% energy bandwidth is defined as the bandwidth which contains 99% of the total energy of the original transmission. Having defined the 99% energy bandwidth, we can investigate how much bandwidth can be saved by discarding 1% of the total transmission energy. In the following, whenever we mention the bandwidth (BW), we mean the 99% energy bandwidth.

In Chapter 2, we have defined the energy of a PRS system as

$$E(\alpha) = \frac{1}{2\pi} \int_{-2\pi\alpha}^{2\pi\alpha} |G(\omega)\ F(\omega)|^2\ d\omega \tag{7.1}$$

where $0 \leq \alpha \leq 1/2T$ Hz.

In this chapter, we consider $G(\omega)$ as an ideal low pass filter of width 1/2T Hz, so $G(\omega)$ is equal to one. Then equation (7.1) becomes

$$E(\alpha) = \frac{1}{2\pi} \int_{-2\pi\alpha}^{2\pi\alpha} |F(\omega)|^2\ d\omega$$

$$= \frac{1}{\pi} \int_{0}^{2\pi\alpha} |F(\omega)|^2\ d\omega \tag{7.2}$$

When $\alpha = 1/2T$ Hz, E will be the total energy of the PRS system and we will have

$$E(\alpha) = \frac{1}{\pi} \int_{0}^{2\pi} |F(\omega)|^2\ d\omega$$

$$= R(0) = \sum_{i=0}^{k-1} f_i^2 \tag{7.3}$$

Let α be the bandwidth that contains 99% of the total energy; then combining (7.2) and (7.3) we have

$$\frac{E(\alpha)}{R(0)} = 0.99 \tag{7.4}$$

which implies

$$\frac{\frac{1}{\pi}\int_0^{2\pi\alpha} F(\omega)^{2}\, d\omega}{\sum_{i=0}^{k-1} fi^2} = 0.99 \tag{7.5}$$

$$\text{or} \quad \frac{1}{\pi}\int_0^{2\pi\alpha} |F(\omega)|^2\, d\omega - 0.99 \left(\sum_{i=0}^{k-1} f_i^2\right) = 0 . \tag{7.6}$$

For instance, when k = 3, we have

$$|F(\omega)|^2 = \left|\sum_{i=0}^{k-1} f_i\, e^{-j\omega iT}\right|^2$$

$$= 1 + f_1^2 + f_2^2 + 2f_2 \cos\omega + 2f_2 f_2 \cos\omega + 2f_2 \cos 2\omega .$$

Substituting $|F(\omega)|^2$ into (7.6), we have

$$\frac{1}{\pi}\int_0^{2\pi\alpha} (1 + f_1^2 + f_2^2 + 2f_1 \cos\omega + 2f_1 f_2 \cos\omega + 2f_2 \cos\omega)\, d\omega$$

$$- 0.99\, (1 + f_1^2 + f_2^2) = 0 \tag{7.7}$$

$$\text{or} \quad (1 + f_1^2 + f_2^2)(2\alpha - 0.99) + \frac{2f_1}{\pi} \sin 2\pi\alpha + \frac{2f_1 f_2}{\pi} \sin 2\pi\alpha$$

$$+ \frac{2f_2}{\pi} \sin 4\pi\alpha = 0 \tag{7.8}$$

A similar computation approach can be applied to other channel lengths as shown in Wong's Appendix [13].

7.2 Minimization of Bandwidth

Before we minimize the bandwidth with degradation (DB) constraint, we first investigate the minimum obtainable bandwidth for channel lengths up to ten. It provides the maximum bandwidth that can be saved when we sacrifice one percent of the total transmission energy.

The problem statement is

$$\begin{aligned} &\text{Min} \quad \alpha \\ &\text{S.T.} \quad \text{(i)} \quad E(\alpha)/R(0) = 0.99 \\ &\qquad\quad \text{(ii)} \quad 0 \leq \alpha \leq \frac{1}{2T} \end{aligned} \tag{7.9}$$

where S.T. means subject to.

This optimisation problem is equivalent to a NLP problem with two inequalities and one equality constraints. To solve this constrained problem, we at first reformulate the constrained NLP problem into an unconstrained minimax problem as described in Chapter 4.

The problem transformation procedure is shown below.

Original defined problem statement :

$$\begin{aligned} &\min \quad \alpha \\ &\text{S.T.} \quad \text{(i)} \quad E(\alpha)/R(0) = 0.99 \\ &\qquad\quad \text{(ii)} \quad 0 \leq \alpha \leq \pi/T \end{aligned} \tag{7.9}$$

$\downarrow$

A NLP problem with four inequality constraints with the form $g_i \geq 0$ $i=1, \ldots 4$.	:	$\min \alpha$ S.T. (i) $E(\alpha)-0.99R(0) \geq 0$ (ii) $-(E(\alpha)-0.99R(0)) \geq 0$ (iii) $\alpha \geq 0$ (7.10) (iv) $1/2T - \alpha \geq 0$
An unconstrained minimax problem.	:	$\min \max\{\alpha, \alpha - \gamma_i g_i\}$ (7.11) where g_i are the four inequality constraints in (7.10) γ_i is a positive real number.

The reformulated problem (7.11) can be solved by the application of Flopt 5. We compute the minimum bandwidth for channel lengths up to ten and the results are shown in Table 7.1, where the bandwidth (BW) is normalized by the minimum Nyquist bandwidth 1/2T and multiplied by 100%. For example, BW = 81.6% for k = 2, means that 99% of the energy is confined within 81.6% of the minimum Nyquist bandwidth 1/2T Hz.

7.3 Discussion of the Results

Fig. 7.1 shows the bandwidth (BW) vs. different channel lengths k. It indicates that the BW decreases as the channel length increases. However, the speed of decreasing in BW slows down when k becomes larger. Thus, even if we further extend channel length beyond ten, the minimum obtainable bandwidth BW

K	BW	DB	The minimum bandwidth channel codes F(D)	Error event
2	81.6%	0.	$1+D$	1
3	63.6%	2.21	$1+1.64D+D^2$	$1-D$
4	50.8%	4.06	$1+1.90D+1.90D^2+D^3$	$1-D$
5	42.0%	5.62	$1+1.96D+2.40D^2+1.96D^3+D^4$	$1-D$
6	35.6%	6.96	$1+1.95D+2.61D^2+2.61D^3+1.95D^4+D^5$	$1-D$
7	30.9%	8.48	$1+1.91D+2.66D^2+2.96D^3+2.66D^4+1.91D^5+D^6$	$1-D-D^2+D^3+D^4-D^5$
8	27.2%	10.24	$1+1.86D+2.64D^2+3.11D^3+3.11D^4+2.64D^5+1.86D^6+D^7$	$1-D-D^2+D^3+D^4-D^5$
9	24.3%	11.38	$1+1.80D+2.58D^2+3.15D^3+3.36D^4+3.15D^5+2.58D^6+1.80D^7+D^8$	$1-D-D^2+D^3+D^4-D^5$
10	22.0%	12.07	$1+1.75D+2.51D^2+3.13D^3+3.48D^4+3.48D^5+3.13D^6+2.51D^7+1.75D^8+D^9$	$1-D-D^2+D^3+D^4-D^5$

Table 7.1 The minimum bandwidth channel codes

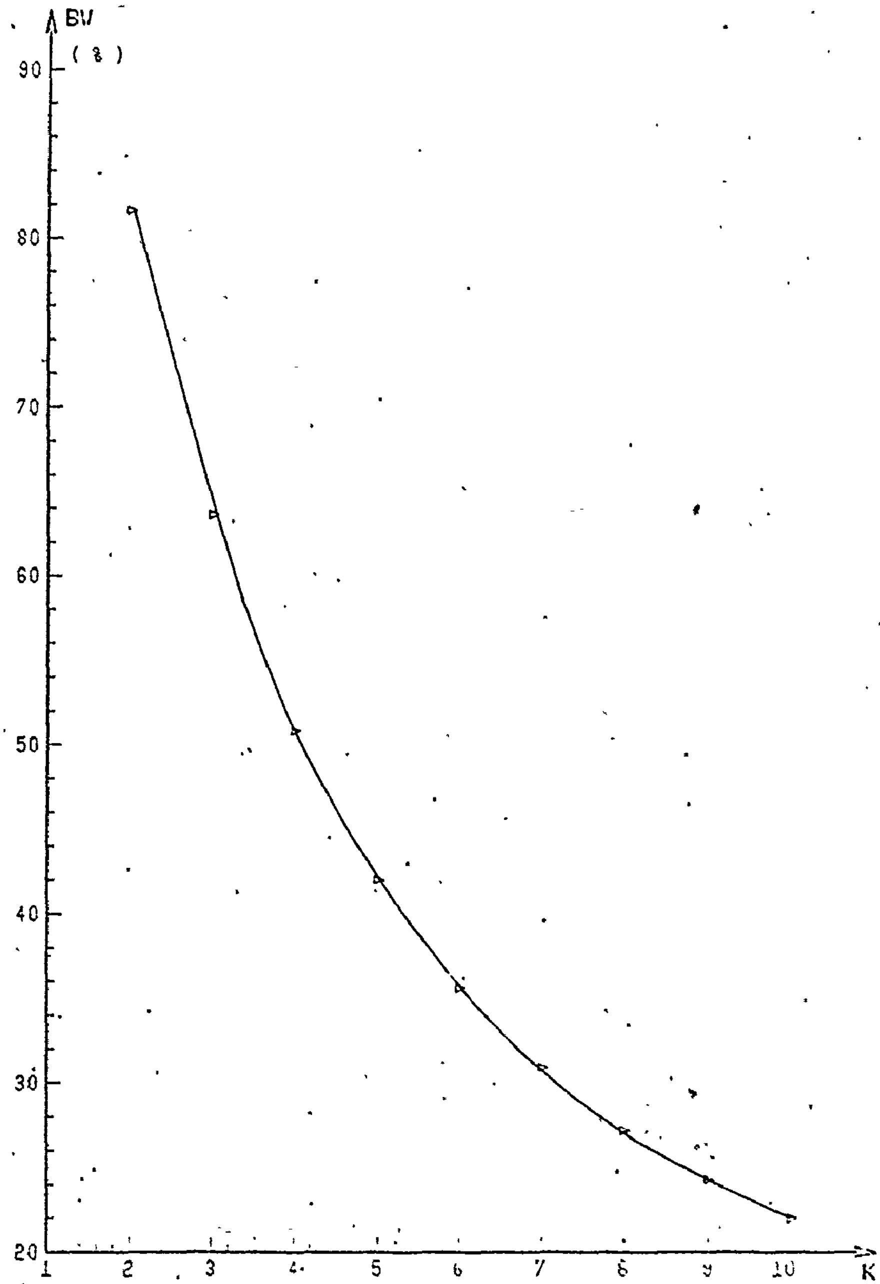

Fig. 7.1 The minimum bandwidth versus channel length

should not be much different from that obtained at k equal to ten.

The higher bandwidth efficiency for a longer channel length can be explained by the locations and number of zeroes of the PRS filter. The zero locations on a Z-plane are shown in Fig. 7.2 for different channel lengths. We observe that all the zeroes are located on the unit circle. As we have mentioned in the last chapter, a zero on a unit circle represents a null in the frequency spectrum, which results in pulling down the energy around the null. Therefore, for a longer channel length, there are more zeroes and thus more nulls, and more energy is suppressed in the higher frequency regions. Fig. 7.3 shows the frequency spectrum of the minimum bandwidth channel codes; it reflects the energy distribution caused by the number of nulls.

When we compare the minimum bandwidth channel codes and the worst-case channel codes obtained in the last chapter, we find that both channel codes have many similar properties. For instance, they are both symmetry about the central tap gain and have all zeroes located on the unit circle. Comparing the degradation in both sets of codes, we see they both suffer nearly the same degradation for the channel lengths less than eight; the difference becomes larger for k greater than or equal to eight. Therefore, if we want to obtain a minimum bandwidth, we have to pay the performance loss nearly equal to the worst-case.

We have seen that the minimum bandwidth codes suffer high degradation for exchange of bandwidth. For instance, when k is

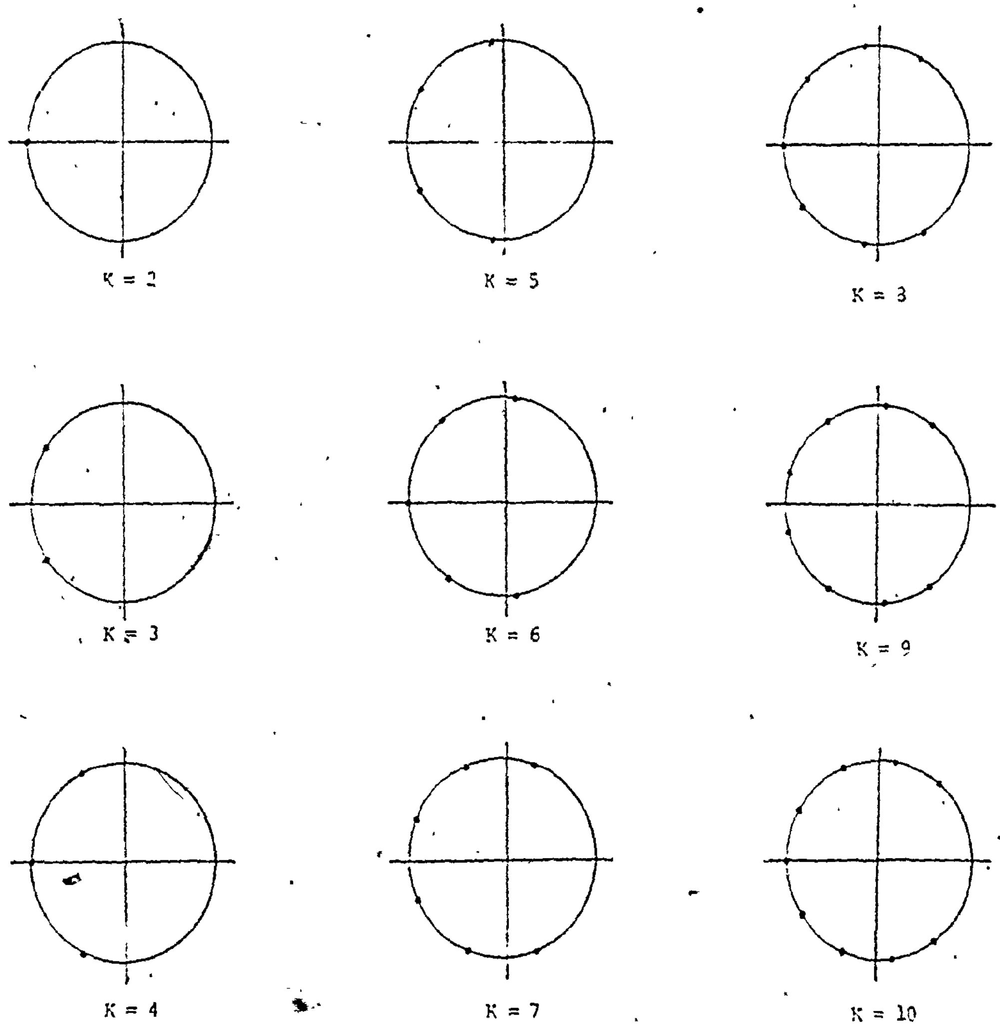

Fig. 7.2 Zero locations in the z-plane for PRG filter with minimum bandwidth .

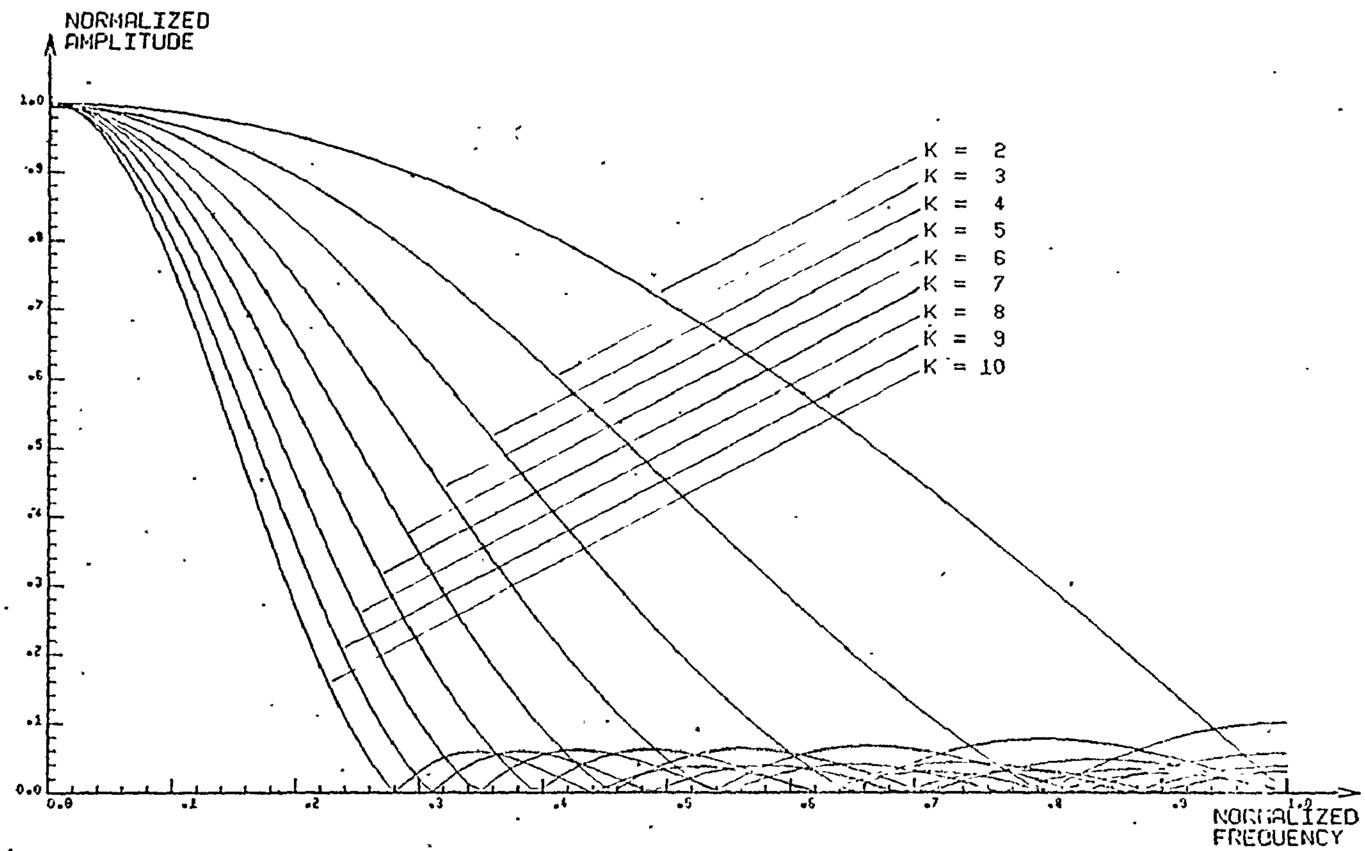

Fig. 7.3 Frequency response of minimum bandwidth PRS filter of channel lengths between 2 to 10.

equal to ten, only 22% of the minimum Nyquist bandwidth is required, but the degradation caused by this channel code is about 12 dB. This may be intolerable. Even if these minimum bandwidth channel codes may not be used in practice, they provide a theoretically obtainable minimum bandwidth of PRS systems with different channel lengths.

7.4 Minimization of Bandwidth with DB Constraint

In the last section, we saw that if we only pay attention to system bandwidth in finding an optimal channel code, noise degradation may be high. Therefore, the consideration of PRS system power is also important, or equivalently the degradation, since degradation can be compensated by increasing the signal power. This can be formulated into a constrained problem of minimizing the bandwidth with fixed noise degradation.

The problem statement is

$$\begin{aligned} &\text{Min} \quad \alpha \\ &\text{S.T.} \quad \text{(i)} \; E(\alpha)/R(0) = 0.99 \\ &\qquad \text{(ii)} \; |DB| \leq C \\ &\qquad \text{(iii)} \; 0 \leq \alpha \leq 1/2T \end{aligned} \tag{7.12}$$

where DB is degradation in dB and C is a positive real number.

Since DB is a function of d^2_{norm}, constraint number two can be converted into the following form.

$$|DB| \leq C$$

is equivalent to $DB \geq C$ since $DB \leq 0$

or $10 \log_{10} (d^2_{norm}/4) \geq C$

or $$d^2_{norm} - 4\,(10^{-0.1C}) \geq 0 \qquad (7.13)$$

This constrained optimisation problem can be first transformed into an unconstrained minimax optimization problem as shown below.

Original problem statement :

$$\begin{aligned} &\text{Min} \quad \alpha \\ &\text{S.T. (i)} \quad E(\alpha)/R(0) = 0.99 \\ &\quad\text{(ii)} \quad |DB| \leq C \\ &\quad\text{(iii)} \quad 0 \leq \alpha \leq \pi/T \end{aligned} \qquad (7.14)$$

An NLP problem with five inequality constraints with the form $g_i \geq 0$, $i=1, \ldots 5$. :

$$\begin{aligned} &\text{Min} \quad \alpha \\ &\text{S.T. (i)} \quad E(\alpha)-0.99R(0) \geq 0 \\ &\quad\text{(ii)} \quad -(E(\alpha)-0.99R(0)) \geq 0 \\ &\quad\text{(iii)} \quad d^2_{norm} - 4(10^{-0.1C}) \geq 0 \\ &\quad\text{(iv)} \quad \alpha \geq 0 \\ &\quad\text{(v)} \quad 1/2T - \alpha \geq 0 \end{aligned} \qquad (7.15)$$

An unconstrained minimax problem :

$$\text{Min max } \{\alpha,\ \alpha - \gamma_i\, g_i\} \qquad (7.16)$$

where g_i are the five inequality constraints shown in (7.15)

γ_i is a positive real number.

The formulated minimax problem is solved by applying the computer package Flopt 5. We have found the minimum bandwidth channel codes with different noise degradation constraints ranging from 1 dB to 6 dB. The computation has been done for channel lengths up to ten. The results are shown in Table 7.2, where DB is the given noise degradation constraint and BW is the minimum bandwidth obtained with the corresponding DB constraint. Various curves of BW vs. DB for channel lengths up to ten are shown in Fig. 7.4, where each point on each curve is the code with minimum bandwidth at a given noise degradation and k.

7.5 Discussion of the Optimal Bandwidth Channel Codes with DB Constraint

The results indicate that there are two different ways to save the bandwidth. First, in a fixed channel length, the bandwidth requirement will be smaller as we loosen the noise degradation constraint. In other words, in order to increase bandwidth efficiency, we can pay for by higher degradation or the performance can be kept by increasing the transmission power. The other way to increase bandwidth efficiency is to increase the channel length. We observe that under the same degradation constraint, the channel with longer constraint length will have better bandwidth performance. It is well known that the complexity of a MLSE receiver increases exponentially as the channel length increases. Thus, this improvement in bandwidth performance is exchanged by increasing the receiver

k	BW	DB	Channel codes F(D)
3	75.96%	1.0	$1+4.583D+3.583D^2$
	71.04%	1.5	$1+2.897D+1.897D^2$
	65.0%	2.0	$1+1.327D+D^2$
4	72.72%	1.0	$1+1.274D-0.05D^2-0.57D^3$
	69.92%	1.5	$1+1.50D+0.403D^2-0.327D^3$
	64.5%	2.0	$1+1.665D+0.93D^2-0.041D^3$
	61.32%	2.5	$1+1.777D+1.176D^2+0.1054D^3$
	58.44%	3.0	$1+1.951D+1.531D^2+0.327D^3$
	54.34%	3.5	$1+2.485D+2.485D^2+D^3$
	51.0%	4.0	$1+1.978D+1.978D^2+D^3$
5	72.48%	1.0	$1-0.57D-3.1316D^2-2.014D^3+0.24D^4$
	69.16%	1.5	$1+1.415D+0.622D^2-0.127D^3+0.09D^4$
	64.32%	2.0	$1+1.627D+0.931D^2-0.054D^3-0.01D^4$
	57.18%	2.5	$1+1.652D+1.287D^2+0.187D^3-0.303D^4$
	55.11%	3.0	$1+1.905D+1.627D^2+0.43D^3-0.242D^4$
	53.21%	3.5	$1+1.965D+1.824D^2+0.73D^3-0.120D^4$
	50.93%	4.0	$1+2.05D+2.065D^2+1.04D^3+0.018D^4$
	48.22%	4.5	$1+2.19D+2.42D^2+1.43D^3+0.247D^4$

Table 7.2(a) The minimum bandwidths with DB contraints for
K = 3 to K = 5

K	BW	DB	Channel codes F(D)
6	71.28%	1.0	$1+2.15D-0.43D^2-2.54D^3-0.75D^4+0.79D^5$
	68.06%	1.5	$1+1.04D-0.62D^2-1.27D^3-0.02D^4+0.55D^5$
	61.63%	2.0	$1+1.66D+1.03D^2+0.02D^3-0.15D^4+0.23D^5$
	57.12%	2.5	$1+1.85D+1.43D^2+0.28D^3-0.35D^4+0.02D^5$
	53.57%	3.0	$1+2.69D+2.47D^2+0.83D^3-0.56D^4-0.52D^5$
	51.03%	3.5	$1+2.00D+1.82D^2+0.66D^3-0.49D^4-0.58D^5$
	48.95%	4.0	$1+1.97D+1.95D^2+1.25D^3+0.09D^4-0.39D^5$
	46.35%	4.5	$1+2.05D+2.22D^2+1.51D^3+0.35D^4-0.29D^5$
	40.4%	6.0	$1+2.25D+2.95D^2+2.58D^3+1.44D^4+0.22D^5$
7	69.77%	1.0	$1+1.22D-0.18D^2-0.84D^3-0.12D^4+0.06D^5-0.27D^6$
	67.92%	1.5	$1+1.23D-0.19D^2-0.97D^3-0.11D^4+0.37D^5-0.04D^6$
	59.1%	2.0	$1+1.68D+1.31D^2+0.04D^3-0.18D^4+0.18D^5+0.46D^6$
	55.02%	2.5	$1+1.98D+1.63D^2+0.37D^3-0.33D^4+0.005D^5+0.31D^6$
	53.1%	3.0	$1+2.05D+1.73D^2+0.46D^3-0.49D^4-0.31D^5+0.13D^6$
	50.04%	3.5	$1+3.38D+3.88D^2+2.19D^3-0.08D^4-1.94D^5-1.31D^6$
	46.26%	4.0	$1+1.88D+1.82D^2+1.06D^3-0.13D^4-0.80D^5-0.58D^6$
	43.31%	4.5	$1+2.05D+2.32D^2+1.73D^3+0.61D^4-0.39D^5-0.55D^6$
	38.91%	6.0	$1+2.03D+2.72D^2+2.45D^3+1.45D^4+0.37D^5-0.26D^6$

Table 7.2(b) The minimum bandwidths with DB contraints for K = 6 and 7.

K	BW	DB	Channel codes F(D)
	69.66%	1.0	$1+0.98D-0.33D^2-0.99D^3-0.19D^4-0.13D^5-0.44D^6-0.18D^7$
	64.34%	1.5	$1+1.58D+0.93D^2-0.13D^3+0.02D^4+0.09D^5-0.23D^6-0.48D^7$
	58.98%	2.0	$1+1.62D+1.24D^2+0.02D^3-0.17D^4+0.20D^5+0.45D^6+0.03D^7$
	54.78%	2.5	$1+2.52D+2.55D^2+0.53D^3-0.52D^4+0.01D^5+0.96D^6+1.00D^7$
8	52.61%	3.0	$1+1.93D+1.54D^2+0.32D^3-0.52D^4-0.19D^5+0.52D^6+0.39D^7$
	49.98%	3.5	$1+2.02D+1.78D^2+0.81D^3-0.55D^4-1.01D^5-0.32D^6-0.02D^7$
	45.29%	4.0	$1+1.93D+1.90D^2+1.24D^3+0.14D^4-0.73D^5-0.53D^6-0.16D^7$
	43.11%	4.5	$1+1.94D+2.09D^2+1.39D^3+0.34D^4-0.56D^5-0.49D^5-0.37D^7$
	37.13%	6.0	$1+1.96D+2.72D^2+2.46D^3+1.75D^4+0.49D^5-0.22D^6-0.51D^7$
	68.0%	1.0	$1+1.09D-0.53D^2-1.09D^3-0.05D^4+0.41D^5+0.03D^6+0.33D^7+0.47D^8$
	64.1%	1.5	$1+2.07D+1.14D^2-0.32D^3-0.60D^4+0.24D^5-0.73D^6-1.28D^7-0.87D^8$
	58.2%	2.0	$1+1.59D+1.13D^2+0.06D^3-0.15D^4+0.13D^5+0.07D^6-0.49D^7-0.35D^8$
	53.8%	2.5	$1+1.93D+1.56D^2+0.33D^3-0.34D^4+0.06D^5+0.55D^6+0.23D^7-0.16D^8$
9	52.1%	3.0	$1+1.91D+1.66D^2+0.62D^3-0.42D^4-0.61D^5-0.26D^6-0.29D^7-0.31D^8$
	49.7%	3.5	$1+1.84D+1.58D^2+0.56D^3-0.59D^4-0.80D^5-0.34D^6-0.15D^7-0.11D^8$
	45.06%	4.0	$1+1.93D+1.93D^2+1.34D^3+0.17D^4-0.77D^5-0.64D^6-0.15D^7+0.05D^8$
	42.45%	4.5	$1+1.85D+2.04D^2+1.39D^3+0.36D^4-0.63D^5-0.57D^6-0.30D^7-0.01D^8$
	35.8%	6.0	$1+2.33D+3.04D^2+3.24D^3+2.24D^4+1.21D^5-0.16D^6-0.80D^7-0.40D^8$

Table 7.2(c) The minimum bandwidths with DB contraints for K = 8 and 9.

K	BW	DB	Channel codes F(D)
	67.2%	1.0	$1+1.73D+0.10D^2-1.36D^3-0.63D^4+0.47D^5-0.29D^6+0.03D^7+0.85D^8+0.91D^9$
	63.3%	1.5	$1+1.15D+0.03D^2-1.07D^3-0.51D^4-0.16D^5-0.71D^6-0.75D^7+0.05D^8+0.44D^9$
	57.86%	2.0	$1+1.53D+1.22D^2+0.07D^3-0.20D^4+0.20D^5+0.16D^6-0.36D^7-0.40D^8-0.11D^9$
	52.7%	2.5	$1+1.84D+1.54D^2+0.29D^3-0.27D^4+0.11D^5+0.56D^6+0.33D^7-0.42D^8-0.41D^9$
10	51.6%	3.0	$1+2.04D+1.88D^2+0.85D^3-0.21D^4-0.31D^5+0.04D^6+0.08D^7-0.41D^8-0.59D^9$
	49.1%	3,5	$1+1.84D+1.68D^2+0.82D^3-0.18D^4-0.57D^5-0.41D^6-0.17D^7-0.24D^8-0.35D^9$
	45.05%	4.0	$1+2.00D+2.02D^2+1.40D^3+0.20D^4-0.84D^5-0.66D^6-0.14D^7+0.05D^8+0.07D^9$
	41.8%	4.5	$1+1.88D+2.01D^2+1.40D^3+0.30D^4-0.73D^5-0.71D^6-0.22D^7+0.19D^8+0.24D^9$
	34.66%	6.0	$1+1.62D+2.15D^2+1.96D^3+1.38D^4+0.20D^5-0.57D^6-0.97D^7-0.70D^8-0.30D^9$

Table 7.2(d) The minimum bandwidths with DB constraints for K = 10.

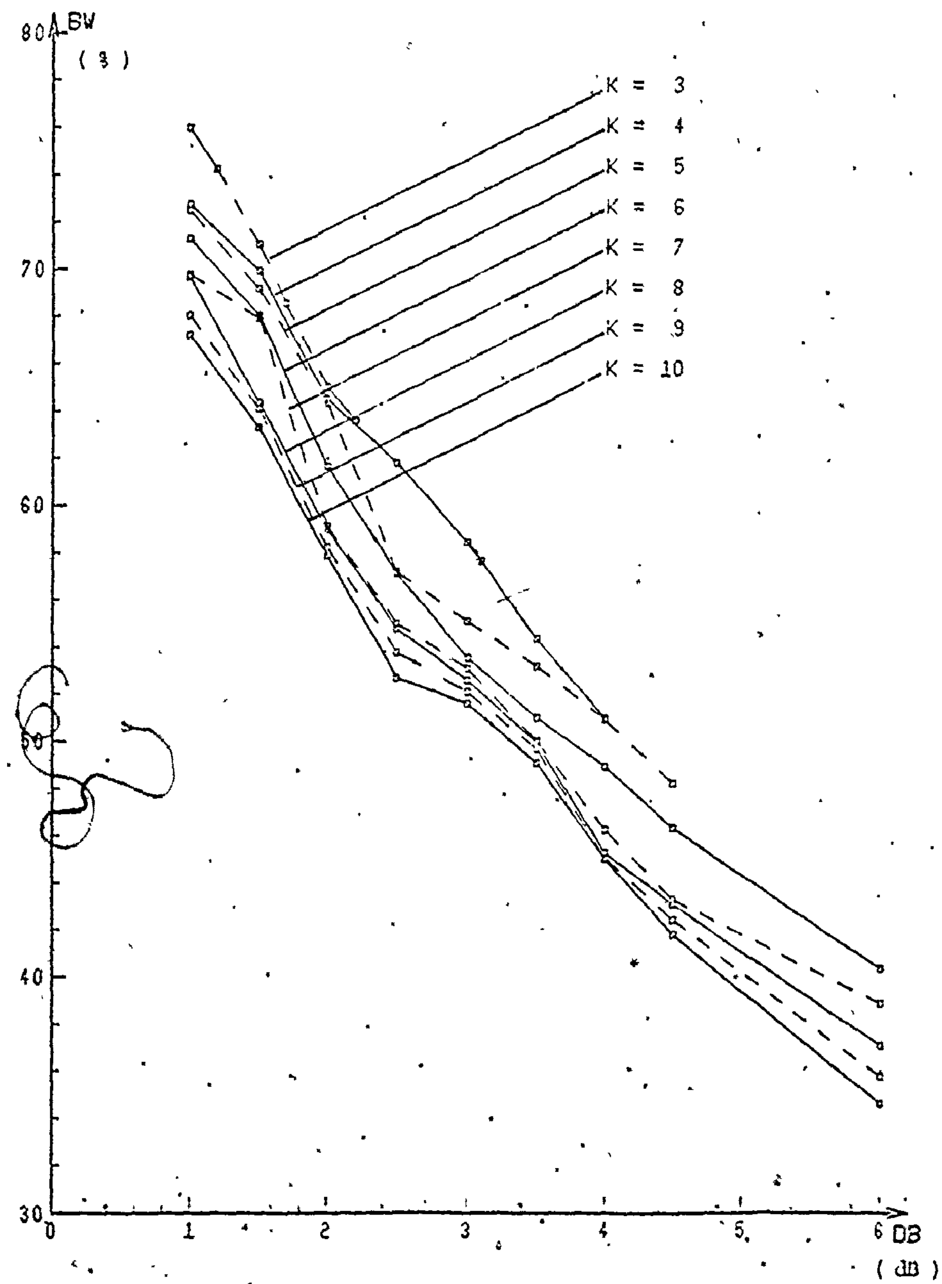

Fig. 7.4 The minimum bandwidth versus degradation for different channel lengths.

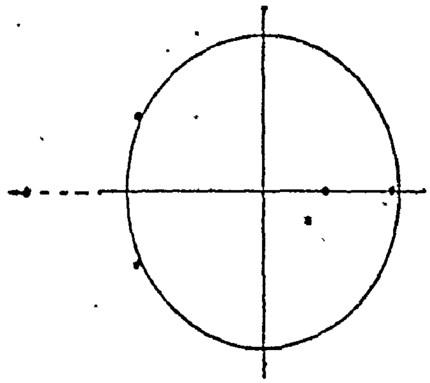

K = 6,

DB constraint = 1.0dB.

Zeroes = -1.81, 0.96, 0.45,
-0.38$\pm$ j0.48.

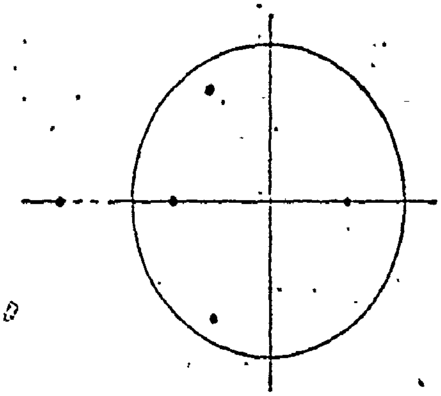

K = 6,

DB constraint = 3.0dB.

Zeroes = -1.44, -0.85, 0.52,
-0.46$\pm$ j0.77.

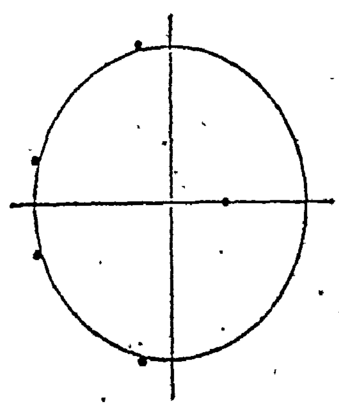

K = 6,

DB constraint = 4.0dB.

Zeroes = -0.95$\pm$ j0.302, 0.338
-0.23$\pm$ j0.974.

Fig. 7.5 Zero locations in Z-plane for PRS filter complexity. However, Fig. 7.4 shows that at some region, even if we increase the channel length, the bandwidth efficiency will not be improved significantly. For instance, the minimum bandwidths are nearly the same at 4 dB noise degradation for channel lengths between eight to ten. In general, the improvement in bandwidth performance becomes smaller as k increases.

Fig. 7.5 shows the zero locations on Z-plane of some of the optimal channel filters found in this section. Unlike the worst-case channel codes or the minimum bandwidth channel codes, the zeroes are not all located on the unit circle. Some of the zeroes are located closely on the unit circle and some may be located far inside or outside the unit circle, and the locations change for the channel codes with different degradation constraints. However, in general, for a fixed channel length more zeroes will locate on the left-hand Z-plane and more will be closed to the circumference when the degradation constraint is loosened. This will pull down the amplutide response at the higher frequency region and make the PRS system require less bandwidth.

We have mentioned that when a receiver is of the structure suggested by Forney [5], a whitening filter is required. The transfer function of the whitening filter is the inverse of the transmitting filter $F(\omega)$, i.e. $1/F(\omega)$. We have found that some of the optimal codes obtained in the last section have zeroes located outside the unit circle. In other words, the whitening filter will have some poles located outside the unit circle and results in an unstable system. From this point-of-view, Forney's receiver structure cannot be applied for some of the channel codes. This is one of the reasons why we consider Ungerboeck's receiver structure [4], which requires no whitening filter.

CHAPTER 8

CONSIDERATION OF RAISED-COSINE FUNCTION FOR PULSE SHAPING

In the previous chapters, all the optimization is done under the assumption that the pulsing shaping filter of the PRS system is a minimum Nyquist bandwidth filter, or equivalently an ideal low pass filter (LPF) with one-side bandwidth 1/2T Hz. However, an ideal LPF is not only unrealizable but also undesirable for pulse shaping because of the slow decay of the pulse tail in the time domain. Serious ISI may result for a small timing error.

In this chapter, we consider a spectral raised-cosine function as the pulse shaping filter of the PRS system. The performance is evaluated and compared with the results obtained in the previous two chapters. The raised-cosine function is chosen because it satisfies Nyquist first criterion and has a very fast decaying pulse tail, resulting in less sensitivity to timing error in a synchronous communication system.

8.1 Bandwidth of a PRS System with the Raised-Cosine Filter

We have mentioned that a PRS system can be considered as a transmitting filter $F(\omega)$ cascades with a pulse shaping filter $G(\omega)$. $F(\omega)$ is a periodic function with period $1/T$. Therefore, with different choice of $G(\omega)$, the PRS system bandwidth will be changed accordingly.

The raised-cosine function consists of a flat amplitude portion and a roll-off portion that has a sinusoidal form, as defined in Chapter 2.

$$G(\omega) \triangleq \begin{cases} T & 0 \leq |\omega| \leq \pi/T\ (1-\beta) \\ T/2\ \{1-\sin[T/2\beta(\omega-\pi/T)]\} & \pi/T\ (1-\beta) \leq |\omega| \leq \pi/T\ (1+\beta) \\ 0 & \text{Otherwise} \end{cases} \quad (8.1)$$

with impulse response

$$g(t) = \frac{\sin \pi t/T}{\pi t/T} \cdot \frac{\cos \beta\pi t/T}{1-4\beta^2 t^2/T} \quad (8.2)$$

Here, we only consider the roll-off factor $\beta = 1$, then $G(\omega)$ is called 100% roll-off and $G(\omega)$ becomes

$$G(\omega) = \begin{cases} T/2\ (1+\cos \omega T/2) & 0 \leq |\omega| \leq 2\pi/T \\ 0 & \text{Otherwise} \end{cases} \quad (8.3)$$

Therefore, the total system bandwidth is $2\pi/T$, twice as that of a PRS system using an ideal LPF with minimum Nyquist bandwidth.

However, the energy distribution of a PRS system is most concentrated in certain frequency regions and in our work, we design the PRS filter that has most energy in the low frequency region. From the viewpoint of 99% energy bandwidth, a PRS system using a raised-cosine function may not necessarily have twice the bandwidth (here and in the following, bandwidth will be interpreted as 99% energy bandwidth unless otherwise specified).

Using the definition of energy density of a PRS system, we are going to derive the bandwidth requirement of a PRS filter that uses a raised-cosine filter for pulse shaping. The energy density of a PRS filter $H(\omega)$ is

$$\text{Energy Density} = |H(\omega)|^2$$
$$= |F(\omega)\ G(\omega)|^2$$
$$= F(\omega)\ \overline{F(\omega)}\ G(\omega)\ \overline{G(\omega)}$$
$$= (1 + \sum_{k=1}^{K-1} f_k\ e^{-j\omega kT})\ (1 + \sum_{k=1}^{K-1} f_k\ e^{j\omega kT}) \cdot$$
$$[T/2\ (1 + \cos\ \omega T/2)]^2. \qquad (8.4)$$

The energy within the frequency band $|\alpha'|$ is

$$E(\alpha') = \frac{1}{\pi} \int_0^{2\pi\alpha'} |H(\omega)|^2\ d\omega\ . \qquad (8.5)$$

Substituting (8.4) into (8.5) and taking the example of k=2, then the energy within $|\alpha'|$ of a PRS filter with $F(\omega)$ having two taps is [Appendix A].

$$E = \frac{1}{\pi} \int_0^{2\pi\alpha'} (1+f_1 e^{-j\omega T})\ (1+f_1 e^{j\omega T})\ [T/2(1+\cos\omega T/2)]^2\ d\omega$$

$$= \frac{3}{4}\ (1+f_1^{\ 2})\ \alpha' + \frac{1}{4}\ f_1\alpha' + (1+f_1^{\ 2}+f_1)\ \frac{\sin\pi\alpha'}{\pi}$$

$$+ [1/8(1+f_1^{\ 2}) + 3/4\ f_1]\ \frac{\sin2\pi\alpha'}{\pi} + \frac{1}{3}\ f_1\ \frac{\sin3\pi\alpha'}{\pi} + \frac{1}{16}\ f_1\ \frac{\sin4\pi\alpha'}{\pi} \qquad (8.6)$$

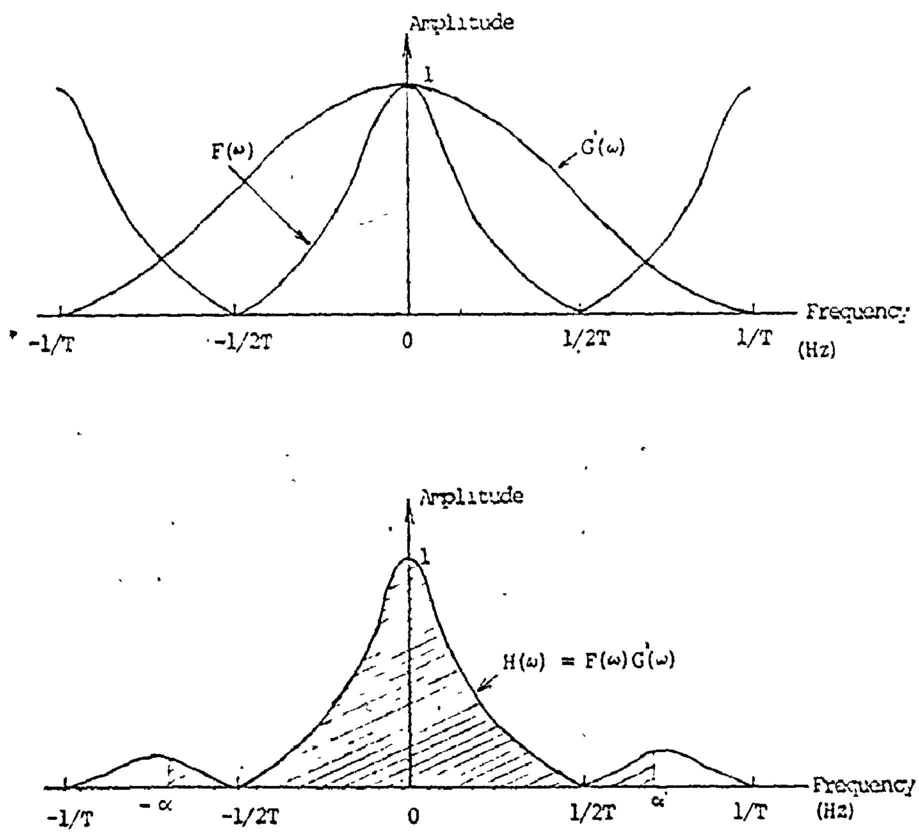

α' -- 99% energy bandwidth

G'(ω) -- raised-cosine function

F(ω) -- digital transversal filter

Fig. 8.1 99% energy bandwidth of a PRS system using a raised-cosine filter.

The total energy R(0) of the PRS system is found by substituting $\alpha'=1$ into (8.6),

$$R(0) = \frac{3}{4}\,(1+f_1^{\,2}) + \frac{1}{4}\,f_1 \tag{8.7}$$

Fig. 8.1 shows the idea of 99% energy bandwidth of a PRS system with a raised-cosine function.

8.2 Minimum Bandwidth of the PRS System with A Raised-Cosine Filter

The 99% energy bandwidth is defined as

$$\frac{E(\alpha')}{R(0)} = 0.99$$

or $E(\alpha')-0.99\,R(0) = 0$ (8.8)

Substituting (8.6) and (8.7) into (8.8), we have

$$[3/4\,(1+f_1^{\,2}) + 1/4\,f_1]\,[\alpha'-0.99] + [(1+f_1^{\,2}) + f_1]\,\frac{\sin\pi\alpha'}{\pi}$$

$$+ [1/8\,(1+f_1^{\,2}) + 3/4\,f_1]\,\frac{\sin 2\pi\alpha'}{\pi} + 1/3\,f_1\,\frac{\sin 3\pi\alpha'}{\pi} + 1/16\,f_1\,\frac{\sin 4\pi\alpha'}{\pi} = 0 \tag{8.9}$$

Now, we want to find the minimum bandwidth α' such that (8.9) holds. It is the same optimisation problem as defined in section 7.2 but with different function definitions.

The optimisation problem is.

$$\begin{aligned}
&\text{Min} \quad \alpha' \\
&\text{Subject to} \quad \text{(i)} \quad E(\alpha')-0.99R(0) \geq 0 \\
&\qquad\qquad\quad \text{(ii)} \quad -(E(\alpha')-0.99\,R(0)) \geq 0 \\
&\qquad\qquad\quad \text{(iii)} \quad \alpha' \geq 0 \\
&\qquad\qquad\quad \text{(iv)} \quad 1/T - \alpha' \geq 0
\end{aligned} \tag{8.10}$$

which is equivalent to the minimax problem ,

$$\text{Min} \quad \text{Max} \quad \{\alpha', \alpha' - \gamma_i\, g_i\} \tag{8.11}$$

where g_i are the four inequality constraints in (8.10), $i=1, \ldots 4$.

With application of Flopt 5, we computed the minimum bandwidth for the PRS filter with k=2 to k=4, where k is the number of tap coefficients of the transmitting filter $F(\omega)$.

The results are shown in Table 8.1. Here we use α' and α to represent the minimum bandwidth obtained by two different PRS filters respectively; α' is obtained by a PRS system using a raised-cosine function while α is obtained by a PRS system with an ideal LPF. The same convention will be used in the following section too.

We observe that all the transmitting filter codes are symmetric about the central tap and the longer codes require less bandwidth; these are the same properties that we have found in section 7.2. The properties can be again explained by the zero locations on the Z-plane. The zeroes of the minimum bandwidth channel filters are all located on the unit circle respectively as shown in Fig. 8.2. More zeroes imply further suppression of the amplitude at higher frequency regions and result in less bandwidth requirement.

K	α'	α	F(D)	$\frac{\alpha'-\alpha}{\alpha}*100\%$
2	0.6447	0.408	$1+D$	58.1%
3	0.3191	0.318	$1+1.59D+D^2$	0.35%
4	0.2466	0.254	$1+1.78D+1.78D^2+D^3$	-2.91%

α' -- minimum bandwidth of a PRS system with a raised-cosine filter.

α -- minimum bandwidth of a PRS system with an ideal low pass filter.

Table 8.1 Minimum bandwidth and the corresponding F(D) codes.

K	F(D)	DB' (raised-cosine)	DB (ideal LPF)	$\frac{DB'-DB}{DB}*100\%$
2	$1+D$	0.67	0.	∞ %
3	$1+1.65D+D^2$	2.682	2.2	21.91%
	$1+1.827D+D^2$	2.495	2.0	24.75%
	$1+2.34D+1.34D^2$	2.232	1.7	31.31%
	$1+2.897D+1.897D^2$	2.058	1.5	37.2%
	$1+3.78D+2.78D^2$	1.793	1.2	49.4%
	$1+4.53D+2.48D^2$	1.612	1.0	61.2%
4	$1+1.98D+1.98D^2+D^3$	4.357	4.0	8.93%
	$1+2.48D+2.48D^2+D^3$	3.876	3.5	10.74%
	$1+1.96D+1.53D^2+0.33D^3$	3.430	3.0	14.74%
	$1+1.73D+1.18D^2+0.1D^3$	2.964	2.5	18.6%
	$1+1.66D+0.93D^2-0.04D^3$	2.491	2.0	24.55%
	$1+1.50D+0.423D^2-0.33D^3$	1.877	1.5	25.13%
	$1+1.27D-0.05D^2-0.57D^3$	1.546	1.0	54.6%

Table 8.2 Comparison of degradation in two different PRS systems with the same F(D) codes

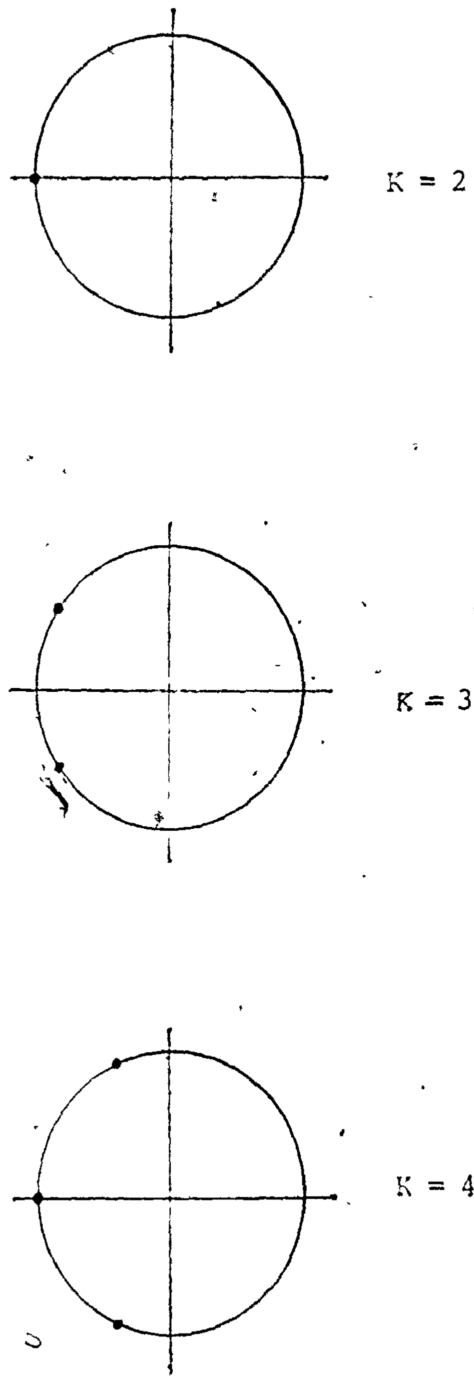

Fig. 8.2 Zero locations in the Z-plane for the PRS filter with minimum bandwidth.

When we compare the two sets of minimum bandwidths α' and α, we observe some interesting results. For k equal to two and three, α' are greater than α, although α' is nearly equal to α for k=3. For k=4, α' becomes smaller than α and we can expect that this is also true for k greater than four. At the beginning of this chapter, we said that the raised cosine function $G'(\omega)$ has twice the minimum Nyquist bandwidth, so we expect that this PRS system will require more bandwidth than the PRS system using an ideal LPF of minimum Nyquist bandwidth. Thus, the results shown here seem to give a little surprise. When we take a close look to the characteristic of the $F(\omega)$ and the raised cosine filter $G'(\omega)$, the results can be explained.

Since the transmitting filter $F(\omega)$ is designed to concentrate most of the energy in the low frequencies in order to narrow the bandwidth, $F(\omega)$ will have frequency response similar to a low pass filter. The raised-cosine function $G'(\omega)$ has low amplitude response in higher frequencies but does have excess bandwidth. The frequency response of the PRS system is $H(\omega) = F(\omega)\ G(\omega)$, which has relatively little amplitude at higher frequencies, but the amount of suppression greatly depends on $F(\omega)$ because of the second "replica" in the spectrum of the discrete $F(\omega)$. When $F(\omega)$ has longer memory, $F(\omega)$ can have a very narrow band in the low frequencies, and the excess bandwidth of $G(\omega)$ will then have little effect and the roll-off characteristic of $G(\omega)$ can help to further suppress the amplitude at the high frequencies. As a result, the bandwidth of this PRS system can be even smaller than that of a PRS filter using an ideal LPF with minimum Nyquist bandwidth.

8.3 Degradation of the PRS System

In the last section, we have seen that a PRS system using a raised-cosine function can have better bandwidth performance than that of a PRS system using an ideal LPF when the transmitting filter has memory longer than three. However, the results should not be overemphasized before we investigate the degradation caused by such two systems because ISI degradation is crucial to the system as well.

The excess bandwidth of the raised-cosine function will introduce aliasing when the outputs of the system are sampled at the symbol rate. This will result in degradation.

The definition of degradation was defined in Sec. 6.1 and it is a function of d^2_{free} and the system energy. When an ideal LPF with minimum Nyquist bandwidth is used in a PRS system, the degradation caused by ISI will originate only in the transmitting filter $F(\omega)$, and the ideal LPF $G(\omega)$ has no effect. Hence, when we compute the degradation or equivalently the normalized d^2_{free}, only $F(\omega)$ needed to be considered. When a PRS system uses a raised-cosine filter $G'(\omega)$ for pulse shaping, the degradation caused by the ISI is not only dependent on $F(\omega)$ but also depends on the aliasing caused by $G'(\omega)$. As a result, the algorithm derived in Chapter 4 to find d^2_{free} cannot be applied to this system because the algorithm is based on the assumption that all the ISI are introduced by $F(\omega)$ only.

To find the degradation of this particular system, we have to consider the characteristic of the whole system function. Equation (3.30) defines the minimum square distance that is a function of input error sequences and the autocorrelation function s_ℓ. s_ℓ is defined in (3.5) and it characterizes the discrete nature of the system. It also reflects the constraint length L of the total ISI of the system; it means $s_\ell = 0$, for $|\ell| > L$. Since we assume that the transfer function of the PRS filter is known, we can find $\{s_\ell\}$ by using (3.5). Therefore, we can apply (3.30) to find the d^2_{free} of this system.

Rewrite the definition of s_ℓ

$$s_\ell \triangleq g_{MF}(t) * h(t)\big|_{t=\ell T}$$

$$= F^{-1}\left(G_{MF}(\omega)\, H(\omega)\right)\big|_{t=\ell T} \tag{8.12}$$

where $H(\omega) = F(\omega)\, G'(\omega) \qquad 0 \le |\omega| \le 2\pi/T$

$$= \left(1 + \sum_{k=1}^{K-1} f_k\, e^{-j\omega kT}\right)(T/2 \cos \omega T/2) \tag{8.13}$$

$$G_{MF}(\omega) = \overline{H}(\omega)$$

$$= \left(1 + \sum_{k=1}^{K-1} f_k\, e^{j\omega kT}\right)(T/2 \cos \omega T/2) \tag{8.14}$$

Then

$$s_\ell = F^{-1}\left\{\left(1 + \sum_{k=1}^{K-1} f_k\, e^{j\omega T}\right)(T/2 \cos \omega T/2)\left(1 + \sum_{k=1}^{K-1} f_k\, e^{-j\omega kT}\right)\cdot (T/2 \cos \omega T/2)\right\}\big|_{t-\ell T} \tag{8.15}$$

If $F(\omega)$ has two taps, K=2, we have

$$F(\omega) = 1 + \sum_{k=1}^{1} f_k \, e^{-j\omega kT}$$

$$= 1 + f_1 \, e^{-j\omega T}.$$

Using (8.15) we find $\{s_\ell\}$ for k=2 are [Appendix B].

$$s_0 = \frac{3}{4}(1 + f_1^2) + \frac{1}{4} f_1$$

$$s_1 = s_{-1} = \frac{3}{4} f_1 + \frac{1}{8}(f_1^2 + 1)$$

$$s_2 = s_{-2} = f_1/8$$

$$s_\ell = 0 \quad \text{for } |\ell| > 2 \ .$$

These results indicate that the constraint length of the ISI is equal to 2 for a PRS system using a raised-cosine function, while it is one for a PRS system using an ideal LPF. In other words, when the raised-cosine function is applied to a PRS system, it may suffer more degradation from the longer ISI that is introduced. This is also true for other channel lengths; the autocorrelation function $\{s_\ell\}$ for different constraint lengths are shown in Appendix B.

Rewrite the definition of d^2_{free};

$$d^2_{free} \stackrel{\Delta}{=} \min_{\varepsilon} \left\{ \sum_{i=0}^{H} \sum_{k=0}^{H} e_i \, s_{i-k} \, e_k \right\} . \tag{8.16}$$

We can apply (8.16) to compute d^2_{free} as soon as we know $\{s_\ell\}$. This is done by searching on an error sequence tree as shown in Fig.

8:3. Here each branch corresponds to an element of a possible error sequence. The tree with depth N can represent all possible error sequences with length less than or equal to N. Searching on the error tree, we compute the resulting distancesof all possible error events and select the sequence with minimum distance, as the error event that causes d^2_{free}. This method is only suitable for a small N due to exponentially growth of the error tree. In this work, we use it to compute d^2_{free} for K less than five, assuming N is equal to five. In other words, we assume the error sequence that causes d^2_{free}, will not be longer than five error intervals. This assumption is acceptable for a short channel length since from previous experience, we observe that the error sequences resulting in d^2_{free} are rarely greater than three for channel lengths less than 5.

In order to show whether this PRS system suffers more degradation than that of a PRS system using an ideal LPF, we compute the degradations (DB) of the two PRS systems with the same $F(\omega)$ and compare the results; see Table 8.2. The results show that under the same $F(\omega)$, the raised-cosine PRS system must suffer more degradation. For a worse degradation channel code, the percentage of difference in degradation between the two PRS systems becomes smaller, and the longer channel length, the smaller percentage difference in DB. Therefore, we expect for a longer channel code or a low bandwidth/high degradation channel codes, the difference in power performance of the two PRS systems will become smaller.

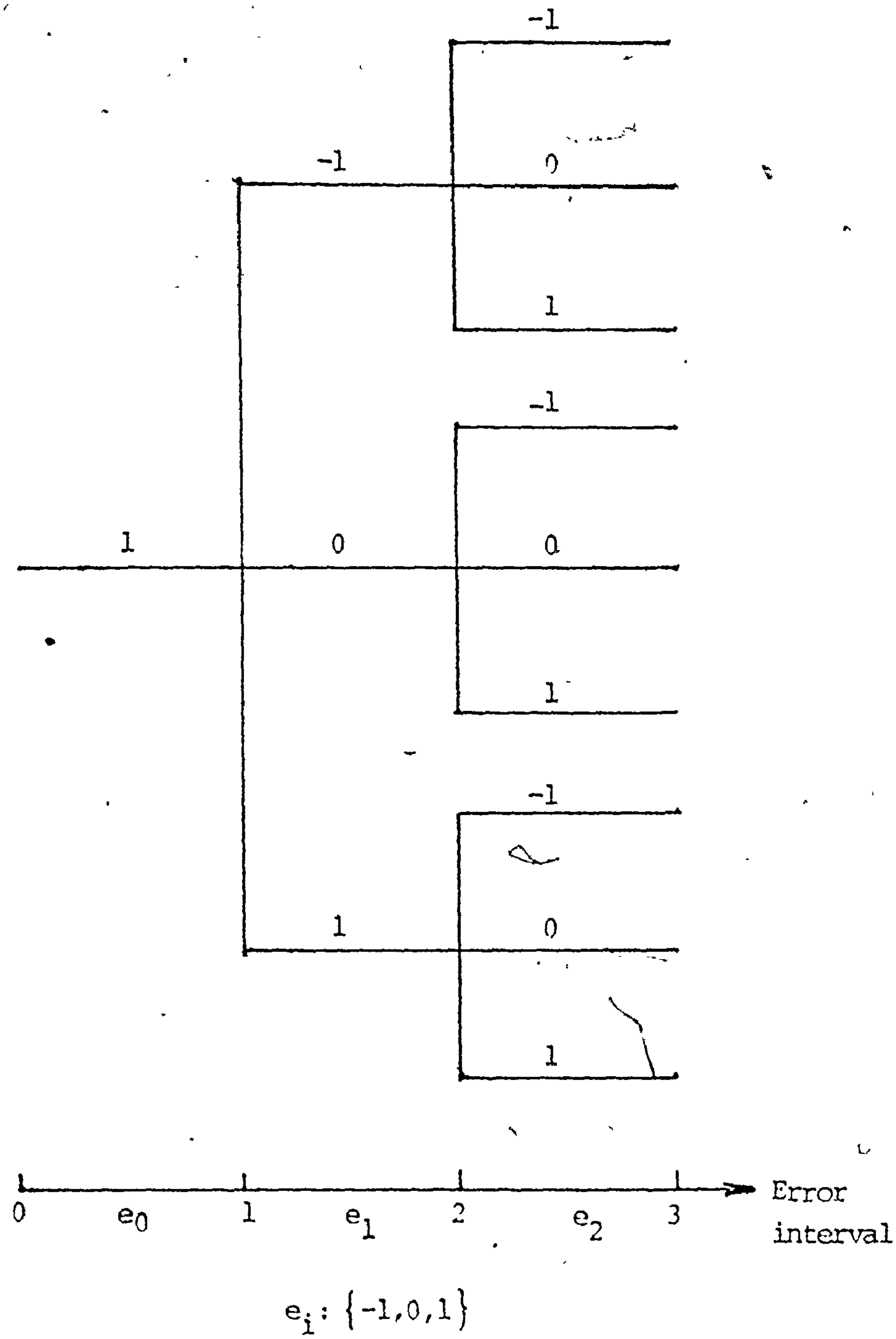

Fig.8.3 An error tree with depth equal to 3

8.4 The Worst Possible Degradation

To find the worst degradation is equivalent to solve an unconstrained optimisation problem defined in section 6.2.

The problem statement is

$$\begin{aligned} &\max_{fi} \{DB\} \\ \equiv &\min_{fi} \{d^2_{norm}\} . \end{aligned} \tag{8.19}$$

Using Flopt 5 and the same techniques discussed in section 6.2, we have found the worst degradation for $k \leq 4$. The results are shown in Table 8.3.

We observe that the error event 1-D causes the worst degradation. All the transmitting filter F(D) codes have the symmetry property and the zeroes of those filters are all located on the unit circle. Moreover, a longer channel length causes worse degradation than a shorter channel length. All the above properties of the worst-case codes are the same as those of a PRS system with an ideal LPF in section 6.2. However, the two different PRS systems have different worst degradation channel codes and different degradations too. As what we expect, the raised-cosine PRS system has worse worst degradation than an ideal LPF PRS system.

8.5 Minimization of Bandwidth with Degradation Constraint

Here we will minimize the bandwidths with different degradation constraints. It is equivalent to solve a constrained optimization problem that has been formulated in section 7.4. Setting up

K	DB'	DB	F(D)	Error event
2	0.67	0.	$1+D$	$1-D$
3	2.88	2.32	$1+1.308D+D^2$	$1-D$
4	4.64	4.13	$1+1.486D+1.486D^2+D^3$	$1-D$

DB' — the worst degradation for a PRS system using a raised-cosine filter.

DB — the worst degradation for a PRS system using an ideal low pass filter.

Table 8.3 The worst degradation for different channel length

K	Optimal α'	DB contraint	F(D)	α^*	$\frac{\alpha'-\alpha}{\alpha}*100\%$
3	0.38	2.0	$1+1.482D+D^2$	0.325	16.92%
	0.455	1.5	$1+1.23D+0.235D^2$	0.355	28.17%
	0.579	1.0	$1+0.514D+D^2$	0.38	52.6%
4	0.263	4.0	$1+2.35D+2.35D^2+D^3$	0.255	3.29 %
	0.308	3.0	$1+1.74D+1.173D^2+0.11D^3$	0.292	5.41%
	0.35	2.0	$1+1.805D+0.84D^2-0.132D^3$	0.323	8.36%
	0.445	1.5	$1+1.986D+0.633D^2-0.113D^3$	0.35	27.14%
	0.614	1.0	$1+2.175D+0.523D^2-0.144D^3$	0.364	68.75%

* α is the optimal bandwidth of the corresponding DB contraints of the PRS system with an ideal LPF; the corresponding F(D) are different from those shown here. Please refer Table 7.2

Table 8.4 Minimum bandwidth with different DB contraints for a PRS system using a raised-cosine filter.

the 99% energy bandwidth and degradation constraints, we can write down the problem statement as below.

$$\begin{aligned} &\text{Min} \quad \alpha' \\ &\text{Subject to} \quad \text{(i)} \quad E(\alpha')-0.99R(0) \geq 0 \\ &\qquad\qquad\quad \text{(ii)} \quad -(E(\alpha')-0.99\,R(0)) \geq 0 \\ &\qquad\qquad\quad \text{(iii)} \quad d^2_{norm} - 4\,(10^{-0.1C}) \geq 0 \\ &\qquad\qquad\quad \text{(iv)} \quad \alpha' \geq 0 \\ &\qquad\qquad\quad \text{(v)} \quad 1/T - \alpha' \geq 0 \end{aligned} \tag{8.18}$$

or equivalently

$$\text{Min} \;\; \text{Max}\, \{\alpha', \alpha' - \gamma_i\, g_i\} \qquad i=1, \ldots, 5 \tag{8.19}$$

where g_i are the five inequality constraints in (8.18).

Using Flopt 5 and the same techniques discussed in section 7.4, we have computed the optimal codes for k up to four and the results are shown in Table 8.4. We observe that for a fixed channel length, the bandwidth decreases as degradation increases. The longer codes can obtain better bandwidth performance under the same degradation constraint. Those are the same properties as for the PRS system discussed in section 7.4.

A comparison of the minimum bandwidth obtained with certain degradation constraints between the two different PRS systems is shown in Table 8.4. Computing the percentage difference of bandwidth between the two systems, we find that under the same channel length, the percentage becomes smaller when the degradation constraint allows more degradation. For instance, when k=4 and DB=4 dB, the percentage difference is only 3.29% in comparison to 27.1% for DB=1.5 dB. When we allow higher degradation, we can choose a set of code f_i such that most of the energy concentrates in the low frequencies. This will make the $F(\omega)$ filter have a narrow band and the excess bandwidth of $G'(\omega)$ has less effect on the system. This property is also true for a longer channel length.

On the whole, we ~~find that~~ a PRS system with raised-cosine function has worse performance than the PRS system with an ideal LPF for k less than 4. As the channel length increases, the PRS system with a raised-cosine function becomes more competitive, especially when we allow moderate degradation. In certain senses, for instance minimization of bandwidth without DB constraint, it can even have better bandwidth performance for k greater than 3. Moreover, the system is less sensitive to timing error.

CHAPTER 9

CONCLUSION

In this thesis, we model a digital communication system by a PRS system and a MLSE receiver. Two different pulse shaping filters are considered for the PRS system, first an ideal low pass filter with minimum Nyquist bandwidth and then a raised-cosine function with roll-off factor equal to one.

A modified stack algorithm has been developed to compute the minimum square distance d^2_{free}. The advantage of this algorithm is that the computational time and memory requirement do not exponentially increase as the channel length. This makes it possible to compute d^2_{free} for channel lengths up to twelve.

A numerical optimization method called Nonlinear Programming is introduced as an approach to solve our optimisation problems. Three different optimisation problems were investigated in this work. First, the worst-case ISI degradation and the corresponding channel codes have been found for channel lengths up to twelve. Secondly, minimizations of system bandwidth under the 99% energy constraint have been done for channel lengths up to ten. Thirdly, we find the minimum 99% energy bandwidth and the corresponding optimal channel codes with different degradation constraints for channel lengths up to ten.

The second and third problems are constrained NLP problems. To solve the constrained problem, we at first reformulate it into an unconstrained minimax problem. All the three optimisation problems are solved by the application of the computer package Flopt 5.

The computation results show that the worst degradation increases as the channel length increases. For k=3, the possible loss in power can be at most 2.323 dB; however, when k goes up to twelve the loss increases to 16.37 dB. The difference is 14.07 dB. Some properties of the worst degradation channels are observed. First, they are all symmetrical channel codes and the zeroes of the filters are all located on the unit circle. The error event that causes the worst degradation, is $\varepsilon=1-D$ for k=3, to k=6, while for k=7 to 12, $\varepsilon=1-D-d^2+D^3+D^4-D^5$ is the error event causing the worst degradation.

In the computation of minimum 99% energy bandwidth, we observe that the longer channel length can obtain a smaller minimum 99% energy bandwidth. It requires 81.6% of the minimum Nyquist bandwidth for k=2 and only 22% of the minimum Nyquist bandwidth when k=10. The saving in bandwidth slows down as k increases and when k goes beyond ten, the saving in bandwidth will not be changed very significantly. The properties of the minimum bandwidth channel codes are the same as those of the worst degradation channel codes, perhaps because the minimum bandwidth channel codes are always located near the worst degradation codes. The number of zeroes and their locations on the unit circle give an explanation of the obtained minimum bandwidth of different channel lengths.

In consideration of the importance of both bandwidth and power, we have tried to find the optimal bandwidth with different constraints on ISI degradation. The results reflect that a longer channel always has better bandwidth performance whatever the degradation constraints are, when compared to a shorter channel length. However, the longer channel length usually causes longer decision depth and so the complexity of receiver increases accordingly.

On the whole, to save more bandwidth, we can either increase the channel length or increase the system power. These tradeoffs can be changed according to different applications.

The three optimisation problems are also considered for k up to four in the case of a PRS system using a spectral raised-cosine function for pulse shaping. Since the excess bandwidth of the raised-cosine function causes ISI in addition to that from the transmitting filter, the system usually suffers more degradation when both PRS systems have the same channel code.

The computation of the worst degradation channel of this PRS system shows that the longer channel length can cause worse degradation. All the other properties of the worst-case channel codes of a PRS system with an ideal low pass filter with minimum Nyquist bandwidth are still true. However, the two different PRS systems have two different sets of worst degradation channel codes. The PRS system with a raised-cosine function has worse worst degradation in comparison to the PRS system with an ideal low pass filter, but the difference becomes smaller as k increases.

The minimum bandwidth channel codes also show the same properties as found before. We observe that the PRS system using a raised-cosine function does not need twice the bandwidth of the previous PRS system and even require less bandwidth for k=4 in a minimum bandwidth channel. We can expect this is also true for k > 4. Of course, this is paid for by suffering more degradation.

In consideration of both bandwidth and degradation, this PRS system usually has an overall worse performance in the short channel codes. The difference between the two PRS systems becomes smaller as k becomes larger and the system bandwidth is reduced. Generally speaking, a narrow band system should employ a raised cosine filter.

Due to the large amount of computation required for evaluating the PRS system using a raised-cosine filter, only channel lengths up to four are investigated. However, we can expect that the performance of such system will become better and better as k increases.

In this work, we do not implement the receiver but only assume the receiver structure is the type suggested by Ungerboeck [4]. Even though Forney's receiver structure [5] is more widely known and used in most other literature, we still prefer Ungerboeck's receiver structure. The reasons are that no whitening filter is required and computation is more efficient.

For a multipath channel, the transmission medium usually changes randomly as opposed to the ISI channel considered here in which the channel is time-invariant. An adaptive receiver is usually required for a multipath channel. Since the ISI introduced by the multipath channel changes randomly, it can happen that the channel will have zeroes located outside the unit circle in the Z-plane. If Forney's receiver structure is used, the receiver will fail in a multipath channel because the channel can cause an unstable whitening filter. Therefore, a receiver without whitening filter like the Ungerboeck's receiver structure must be used for the multipath channel. In short, we believe that Ungerboeck's receiver is more practical.

APPENDIX A

Derivation of the Energy of a PRS System with Raised-Cosine Function

For k=2, $F(\omega) = 1 + f_1 e^{-j\omega}$

The energy of the PRS filter is

$$E = \frac{1}{\pi} \int_0^{2\pi\alpha'} |H(\omega)|^2 \, d\omega$$

$$= \frac{1}{\pi} \int_0^{2\pi\alpha'} (1 + f_1 e^{-j\omega}) \, (1 + f_1 e^{j\omega}) \, [\tfrac{1}{2}(1 + \cos\tfrac{\omega}{2})]^2 \, d\omega$$

$$= \frac{1}{\pi} \int_0^{2\pi\alpha'} [1 + f_1^2 + f_1 \, (e^{-j\omega} + e^{j\omega})] \, [\tfrac{1}{4}(1 + 2\cos\tfrac{\omega}{2} + \cos^2 \tfrac{\omega}{2})] \, d\omega$$

$$= \frac{1}{4\pi} \int_0^{2\pi\alpha'} [1 + f_1^2 + 2f_1 \cos\omega + 2\cos\tfrac{\omega}{2} + 2f_1^2\cos\tfrac{\omega}{2} + 4f_1 \cos\tfrac{\omega}{2} \cos\omega$$

$$+ \cos^2 \tfrac{\omega}{2} + f_1^2\cos^2 \tfrac{\omega}{2} + 2f_1 \cos^2 \tfrac{\omega}{2} \cos\omega] \, d\omega$$

$$= \frac{1}{4\pi} \int_0^{2\pi\alpha'} \{(1 + f_1^2 + 2f_1 \cos\omega + 2\cos\tfrac{\omega}{2} + 2f_1^2\cos\tfrac{\omega}{2} + 2f_1(\cos\tfrac{3\omega}{2} + \cos\tfrac{\omega}{2})$$

$$+ \frac{1}{2}(1 + \cos\omega) + \frac{f_1^2}{2}(1 + \cos\omega) + f_1\cos\omega + \frac{f_1}{2}(1 + \cos 2\omega)\} \, d\omega$$

$$= \frac{1}{4\pi} \{ \int_0^{2\pi\alpha'} (1 + f_1^2 + \frac{1}{2} + \frac{f_1^2}{2} + \frac{f_1}{2})\, d\omega + \int_0^{2\pi\alpha'} (2f_1 + \frac{1}{2} + \frac{f_1^2}{2} + f_1) \cos\omega \, d\omega$$

$$+ \int_0^{2\pi\alpha'} (2 + 2f_1^2 + 2f_1) \cos\frac{\omega}{2}\, d\omega + \int_0^{2\pi\alpha'} 2f_1 \cos\frac{3\omega}{2}\, d\omega + \int_0^{2\pi\alpha'} f_1 \cos 2\omega \, d\omega \}$$

$$= \frac{3}{4} (1 + f_1^2)\, \alpha' + \frac{1}{4} f_1 \alpha' + (1 + f_1 + f_1^2) \frac{\sin\pi\alpha'}{\pi} + \frac{1}{8}(1 + 6f_1 + f_1^2)\frac{\sin 2\pi\alpha'}{\pi}$$

$$+ \frac{1}{3} f_1 \frac{\sin 3\pi\alpha'}{\pi} + \frac{f_1}{16\pi} \sin 4\pi\alpha'$$

Using the same approach, we can compute the energy of the PRS system with $k > 2$.

APPENDIX B

Derivation of Autocorrelation Function $\{s_l\}$ for a PRS System with Raised Cosine Function

For k=2, $F(\omega) = 1 + f_1 e^{-j\omega}$

$$G(\omega) = \frac{1}{2}\left(1 + \cos\frac{\omega}{2}\right) \qquad 0 \leq \omega \leq \frac{2\pi}{T}$$

The transfer function of the PRS system is $H(\omega)$

$$H(\omega) = G(\omega)\, F(\omega)$$

$$= \frac{1}{2}\left(1 + \cos\frac{\omega}{2}\right)\left(1 + f_1 e^{-j\omega}\right)$$

The match filter transfer function is $G_{MF}(\omega)$

$$G_{MF}(\omega) = \overline{H}(\omega)$$

$$= \frac{1}{2}\left(1 + \cos\frac{\omega}{2}\right)\left(1 + f_1 e^{j\omega}\right)$$

The signal element s_l is

$$s_l = g_{MF}(t) * h(t)\big|_{t=lT}$$

$$= F^{-1}\left\{G_{MF}(\omega)\, H(\omega)\right\}\big|_{t=lT}$$

$$= F^{-1}\{\frac{1}{4}(1 + 2\cos\frac{\omega}{2} + \cos^2\frac{\omega}{2})(1 + f_1^2 + f_1(e^{-j\omega} + e^{j\omega}))\}|_{t=\ell T}$$

$$= F^{-1}\{\frac{1}{4}(1 + f_1^2 + f_1(e^{-j\omega} + e^{j\omega}) + 2(1 + f_1^2 + f_1(e^{-j\omega} + e^{j\omega})\cdot$$

$$\cos\frac{\omega}{2} + (1 + f_1^2 + f_1(e^{-j\omega} + e^{j\omega}))\cos^2\frac{\omega}{2}\}|_{t=\ell T}$$

$$= \frac{1}{4}\{3(1 + f_1^2)(\frac{\sin 2\pi t/T}{2\pi t/T}) + 3f_1 \frac{\sin(2\pi - 2\pi t/T)}{2\pi - 2\pi t/T}$$

$$+ \frac{1}{2}(1 + f_1^2)[\frac{\sin(2\pi + 2\pi t/T)}{2\pi + 2\pi t/T} + \frac{\sin(2\pi - 2\pi t/T)}{2\pi - 2\pi t/T}]$$

$$+ \frac{f_1}{2}[2\frac{\sin\pi t/T}{2\pi t/T} + \frac{\sin(4\pi - 2\pi t/T)}{4\pi - 2\pi t/T} + \frac{\sin(4\pi + 2\pi t/T)}{4\pi + 2\pi t/T}]\}|_{t=\ell T}$$

$$= \frac{1}{4}\{[3(1 + f_1^2) + f_1]\frac{\sin 2\pi t/T}{2\pi t/T} + [3f_1 + \frac{1}{2}(1 + f_1^2)][\frac{\sin(2\pi + 2\pi t/T)}{2\pi + 2\pi t/T}$$

$$+ \frac{\sin(2\pi - 2\pi t/T)}{2\pi - 2\pi t/T}] + \frac{f_1}{2}[\frac{\sin(4\pi + 2\pi t/T)}{4\pi + 2\pi t/T} + \frac{\sin(4\pi - 2\pi t/T)}{4\pi - 2\pi t/T}]\}|_{t=\ell T}$$

Therefore, for k=2

$$s_0 = \frac{3}{4}(1 + f_1^2) + \frac{1}{4}f_1$$

$$s_1 = s_{-1} = \frac{3}{4}f_1 + \frac{1}{8}(1 + f_1^2).$$

$$s_2 = s_{-2} = \frac{f_1}{8}$$

$$s_\ell = 0, \quad \text{for } |\ell| \geq 3$$

Using the same approach, we can find the signal element s_ℓ for $k > 2$ as shown below.

For k=3

$$s_\ell = \frac{1}{4}\{[3(1 + f_1^2 + f_2^2) + f_1 + f_1f_2]\frac{\sin 2\pi t/T}{2\pi t/T} + [3f_1 + 3f_1f_2 + \frac{f_2 + 1 + f_1^2 + f_2^2}{2}]\cdot$$

$$[\frac{\sin(2\pi+2\ t/T)}{2\pi+2\pi t/T} + \frac{\sin(2\pi-2\pi t/T)}{2\pi-2\pi t/T}] + (3f_2 + \frac{1}{2}f_1 + \frac{1}{2}f_1f_2)\ [\frac{\sin(4\pi+2\pi t/T)}{4\pi+2\pi t/T}$$

$$+ \frac{\sin(4\pi-2\pi t/T)}{4\pi-2\pi t/T}] + \frac{f_2}{2}[\frac{\sin(6\pi+2\pi t/T)}{6\pi+2\pi t/T} + \frac{\sin(6\pi-2\pi t/T)}{6\pi-2\pi t/T}]\}\ \Big|_{t=\ell T}$$

Therefore, for k=3

$$s_0 = \frac{3}{4}(1 + f_1^2 + f_2^2) + \frac{1}{4}(f_1 + f_1f_2)$$

$$s_1 = s_{-1} = \frac{3}{4}(f_1 + f_1f_2) + \frac{1}{8}(1 + f_1^2 + f_2^2) + \frac{1}{8}f_2$$

$$s_2 = s_{-2} = \frac{3}{4}f_2 + \frac{1}{8}(f_1 + f_1f_2)$$

$$s_3 = s_{-3} = \frac{1}{8}f_2$$

$$s_\ell = 0 \quad \text{for} \quad |\ell| \geq 4$$

For k=4

$$s_\ell = \frac{1}{4}\{[3(1 + f_1^2+f_2^2+f_3^2) + (f_1+ f_1f_2+f_2f_3)]\frac{\sin 2\pi t/T}{2\pi t/T} + [3(f_1+f_1f_2+f_2f_3)$$

$$+ \frac{1}{2}(1 + f_1^2+f_2^2+f_3^2) + \frac{1}{2}(f_2+f_1f_3)][\frac{\sin(2\pi+2\pi t/T)}{2\pi+2\pi t/T} + \frac{\sin(2\pi-2\pi t/T)}{2\pi-2\pi t/T}]$$

$$+ [3(f_2+f_1f_3) + \frac{1}{2}(f_1+f_1f_2+f_2f_3) + \frac{1}{2}f_3][\frac{\sin(4\pi+2\pi t/T)}{4\pi+2\pi t/T} +$$

$$\frac{\sin(4\pi-2\pi t/T)}{4\pi-2\pi t/T}] + [3f_3+\frac{1}{2}(f_2+f_1f_3)](\frac{\sin(6\pi+2\pi t/T)}{6\pi+2\pi t/T} + \frac{\sin(6\pi-2\pi t/T)}{6\pi-2\pi t/T}]\}\Big|_{t=\ell T}$$

Therefore, for k=4

$$s_0 = \frac{3}{4}(1 + f_1^2+f_2^2+f_3^2) + \frac{1}{4}(f_1+f_1f_2+f_2f_3)$$

$$s_1 = s_{-1} = \frac{1}{8}(1 + f_1^2+f_2^2+f_3^2) + \frac{3}{4}(f_1+f_1f_2+f_2f_3) + \frac{1}{8}(f_2 + f_1f_3)$$

$$s_2 = s_{-2} = \frac{3}{4}(f_2 + f_1f_3) + \frac{1}{8}(f_1 + f_1f_2+f_2f_3) + \frac{1}{8}(f_3)$$

$$s_3 = s_{-3} = \frac{3}{4}(f_3) + \frac{1}{8}(f_2 + f_1f_3)$$

$$s_4 = s_{-4} = \frac{1}{8}f_3$$

$$s_\ell = 0 \quad \text{for} \quad |\ell| \geq 5$$

REFERENCES

[1] P. Kabal and S. Pasupathy, "Partial-response signaling", IEEE Trans. on Commun., Vol. COM-23, pp. 921-934, Sept. 1975.

[2] R. W. Lucky, J. Salz, and E. J. Weldon, Principles of Data Communications, New York: McGraw-Hill, 1968.

[3] R. Price,"Nonlinearly feedback-equalized PAM vs. capacity for noisy filter channels", 1972 Int. Conf. Commun., Philadelphia, June 1972.

[4] G. Ungerboeck, "Adaptive maximum-likelihood receiver for carrier-modulated data-transmission systems", IEEE Trans. on Commun., Vol. COM-23, pp. 624-636, May 1974.

[5] G. D. Forney, Jr., "Maximum-likelihood sequence estimation of digital sequences in the presence of intersymbol interference", IEEE Trans. on Inform. Theory, Vol. IT-18, pp. 363-378, May 1972.

[6] A. J. Viterbi, "Convolutional codes and their performances in communication systems", IEEE Trans. Commun. Techn., Vol. COM-19, pp. 751-772, Oct. 1971.

[7] J. K. Omura, "On Viterbi decoding algorithm, "IEEE Trans. Inform. Theory, Vol. IT-15, pp. 177-179, Jan. 1969.

[8] H. Kobayashi, "Correlative level coding and maximum-likelihood decoding, "IEEE Trans. Inform. Theory, Vol. IT-19, pp. 586-594, Sept. 1971.

[9] G. D. Forney, Jr., "Lower bounds on error probability in the presence of large intersymbol interference, "IEEE Trans. Commun. Techn. Vol. COM-20, pp. 76-77, Feb. 1972.

[10] F. R. Magee, Jr., and J. G. Proakis, "Adaptive maximum likelihood sequence estimation for digital signal in the presence of intersymbol interference", IEEE Trans. Inform. Theory (Corresp.), Vol. IT-19, pp. 120-124, Jan. 1973.

[11] F. R. Magee, Jr., and J. G. Proakis, "An estimate of the upper bound on error probability for maximum-likelihood sequence estimation on channel having a finite-duration pulse response", IEEE Trans. Inform. Theory, Vol. IT-10, pp. 699-702, Sept. 1973.

[12] R. R. Anderson and G. J. Foschini, "The minimum distance for MLSE digital data system of limited complexity", IEEE Trans. Inform. Theory, Vol. IT-21, pp. 544-551, Sept. 1975.

[13] C. W. C. Wong, "Power, Bandwidth and Complexity in maximum likelihood sequence estimation", Faculty of Engineering, McMaster University, July 1980, Report CRL-78.

[14] A. Lender, "Correlative level coding for binary data transmission", IEEE Spectrum, Vol. 3, pp. 104-115, Feb. 1966.

[15] W. R. Bennett, Introduction to Signal Transmission, New York: McGraw Hill, 1970.

[16] G. D. Forney, Jr., "The Viterbi algorithm", IEEE Proceedings, Vol. 61, pp. 268-278, March 1973.

[17] D. G. Messerschmitt, "A geometric theory of intersymbol interference, part 2: Performance of the maximum-likelihood detector", Bell Syst. Tech. J., Vol. 52, pp. 1521-1539, Nov. 1973.

[18] T. Aulin and C-E Sundberg, "Minimum distance properties of M-ary correlative encoded CPFSK", Technical Report TR-120, Telecommun. Theory, Electrical Eng. Dept., University of Lund, Nov. 1978.

[19] A. J. Viterbi and J. K. Omura, Principles of Digital Communication and Coding, New York: McGraw Hill, 1979.

[20] W. I. Zangwill, Nonlinear Programming: A Unified Approach, Prentice-Hall, Englewood Cliffs, New Jersey, 1969.

[21] H. Sagan, Introduction to the Calculus of Variations, New York: McGraw Hill, 1969.

[22] W. W. Kuhn and A. W. Tucker, "Nonlinear Programming", Proc. 2d Berkeley Symp. on Math. Statistics and Probability, University of California Press, Berkeley 1951.

[23] G. C. Temes and S. K. Mitra, Modern Filter Theory and Design, New York: Wiley, 1973.

[24] A. V. Fiacco and G. P. McCormick, Nonlinear Programming: Sequential Unconstrained Minimization Techniques, New York: Wiley, 1968.

[25] R. Fletcher, "An exact penalty function for nonlinear programming with inequalities", Math. Programming, Vol. 5, pp. 129-150, 1973.

[26] J. W. Bandler and C. Charalambous, "Nonlinear programming using minimax techniques", J. of Opt. Theory and Application, pp. 607-619, Vol. 13, No. 6, 1974.

[27] C. Charalambous, "Nonlinear least pth optimisation and nonlinear programming", Math. Programming, Vol. 12, pp. 195-225, 1977.

[28] C. Charalambous, "Acceleration of the least pth algorithm for minimax optimisation with engineering application", Math. Programming, Vol. 17, pp. 270-297, 1979.

[29] R. Fletcher, "Fortran Subroutines for minimization by quasi-Newton methods", Atomic Energy Research Establishment, Harwell, Berkshire, England, Report A ERZ-R7125, 1972.

[30] J. W. Bandler and D. Sinha, "Flopt 5 - A program for minimax optimisation using the accelerated least pth algorithm", Faculty of Engineering, McMaster University, Dec. 1978, Report SOC-218.

[31] D. G. Messerschmitt, "A geometric theory of intersymbol interference, Part I: Zero-forcing and decision-feedback equalization", Bell Syst. Tech. J., Vol. 52, pp. 1483-1518, Nov. 1973.